

Can graph neural networks count substructures?

Zhengdao Chen^a, Lei Chen^a, Soledad Villar^{a, b}, and Joan Bruna^{a, b, c}

^aCourant Institute of Mathematical Sciences, New York University, New York

^bCenter for Data Science, New York University, New York

^cInstitute for Advanced Study, Princeton

March 24, 2024

Abstract

The ability to detect and count certain substructures in graphs is important for solving many tasks on graph-structured data, especially in the contexts of computational chemistry and biology as well as social network analysis. Inspired by this, we propose to study the expressive power of graph neural networks (GNNs) via their ability to count attributed graph substructures, extending recent works that examine their power in graph isomorphism testing. We distinguish between two types of substructure counting: matching-count and containment-count, and establish mostly negative answers for a wide class of GNN architectures. Specifically, we prove that Message Passing Neural Networks (MPNNs), Weisfeiler-Lehman (WL) and 2-Invariant Graph Networks (2-IGNs) cannot perform matching-count of substructures consisting of 3 or more nodes, while they can perform containment-count of star-shaped substructures. We also provide partial results for k -WL and k -IGNs. We then conduct experiments that support several of the theoretical results, and demonstrate that local relational pooling strategies inspired by [Murphy et al. \(2019\)](#) are more effective for substructure counting. In addition, we prove that WL and 2-IGNs are equivalent in distinguishing non-isomorphic graphs, partly answering an open problem raised in [Maron et al. \(2019a\)](#).

1 Introduction

In the past few years, graph neural networks (GNNs) have achieved empirical success on processing data from various fields such as social networks, quantum chemistry, particle physics, knowledge graphs and combinatorial optimization ([Scarselli et al., 2008](#); [Bruna et al., 2013](#); [Duvenaud et al., 2015](#); [Kipf and Welling, 2016](#); [Defferrard et al., 2016](#); [Bronstein et al., 2017](#); [Dai et al., 2017](#); [Nowak et al., 2017](#); [Ying et al., 2018](#); [Zhou et al., 2018](#); [Choma et al., 2018](#); [Zhang and Chen, 2018](#); [You et al., 2018a,b](#); [Yao et al., 2019](#); [Ding et al., 2019](#)). Thanks to such progress, there has been a recent interest in studying the expressive power of GNNs. One line of work does so by studying their ability to distinguish non-isomorphic graphs. For example, [Xu et al. \(2018a\)](#) and [Morris et al. \(2019\)](#) show that GNNs based on neighborhood-aggregation schemes are at most as powerful as the classical Weisfeiler-Lehman (WL) test ([Weisfeiler and Leman, 1968](#)) in this regard and propose GNN architectures that can achieve such level of power. While graph isomorphism testing is very interesting from a theoretical viewpoint, one may naturally wonder how relevant it is to real-world tasks on graph-structured data. Especially, WL is already quite powerful in the sense that except for counterexamples that are quite rare, almost all pairs of non-isomorphic graphs can be distinguished by WL ([Babai et al., 1980](#)). Hence, from the graph isomorphism testing perspective, existing GNNs are already in some sense not far away from being maximally powerful, which could make the pursuit of more powerful GNNs appear unnecessary.

Another perspective is the ability of GNNs to approximate permutation-invariant functions on graphs. For instance, [Maron et al. \(2019c\)](#) and [Keriven and Peyré \(2019\)](#) propose architectures that achieve universal

approximation of permutation-invariant functions on graphs, though such models involve tensors with order growing in the size of the graph and are therefore impractical. Moreover, [Chen et al. \(2019b\)](#) establishes an equivalence between the ability to distinguish any pair of non-isomorphic graphs and the ability to approximate arbitrary permutation-invariant functions on graphs. Nonetheless, for GNNs used in practice, which are not universally approximating, we still lack a concrete and intuitive understanding of what they can and cannot do. [Loukas \(2019\)](#) takes an interesting direction of showing that GNNs under assumptions are Turing universal but loses power when its depth and width are limited, though the arguments rely on the nodes all having distinct features and the focus is on the asymptotic depth-width tradeoff.

In this paper, inspired by the relevance of detecting and counting *graph substructures* in applications, we propose to understand the power of GNN architectures via the substructures that they can and cannot count. Also referred to by various names including *graphlets*, *motifs*, *subgraphs* and *graph fragments*, graph substructures are well-studied and relevant for graph-related tasks in computational chemistry ([Deshpande et al., 2002](#); [Duvenaud et al., 2015](#); [Jin et al., 2018, 2019](#)), computational biology ([Koyutrk et al., 2004](#)) and social network studies ([Jiang et al., 2010](#)). In organic chemistry, for example, certain patterns of atoms called functional groups are usually considered indicative of the molecules’ properties ([Lemke, 2003](#)). In the literature of molecular chemistry, substructure counts have been used to generate molecular fingerprints ([Morgan, 1965](#); [OBoyle and Sayle, 2016](#)) and computing similarities between molecules ([Alon et al., 2008](#); [Rahman et al., 2009](#)). In addition, graphlet counts have been used to create general-purpose graph kernels ([Shervashidze et al., 2009](#)). The connection between GNNs and graph substructures is explored empirically by [Ying et al. \(2019\)](#) as a way to interpret the predictions made by GNNs. Thus, the ability of different GNN architectures to count graph substructures not only serves as an intuitive theoretical measure of their expressive power but also is highly relevant to real-world scenarios. While people have proposed variants of GNNs that take advantage of substructure information ([Monti et al., 2018](#); [Liu et al., 2018, 2019](#)), often they rely on handcrafting rather than learning such information. More importantly, there is a lack of systematic theoretical study of the ability of classical GNNs to count substructures.

In this work, we first build a theoretical framework for studying the ability of GNNs to count *attributed* substructures based on both function approximation and graph discrimination. In particular, we distinguish between *containment-count* and *matching-count*, each corresponding to having *subgraphs* and *induced subgraphs* isomorphic to a given pattern, respectively. Next, we look at classical GNN architectures and prove the following results.

1. Focusing on matching-count, we establish that neither Message Passing Neural Networks (MPNNs) ([Gilmer et al., 2017](#)) nor 2nd-order Invariant Graph Networks (2-IGNs) ([Maron et al., 2019c](#)) can count any connected substructure of more than 3 nodes. For any such pattern, we prove this by constructing a pair of graphs that provably cannot be distinguished by any MPNN or 2-IGN but with different matching-counts of the given pattern. This result points at an important class of simple-looking tasks that are provably hard for classical GNN architectures.
2. We show positive results for containment-count of star-shaped patterns by MPNNs and 2-IGNs, generalizing results in [Arvind et al. \(2018\)](#), as well as for both matching- and containment-count of size- k patterns by k -WL and k -IGNs. The latter result hints at a hierarchy of the increasing power of k -WL’s in terms of counting substructures, which would be more intuitive than the hierarchy in terms of distinguishing non-isomorphic graphs as shown in [Cai et al. \(1992\)](#), and therefore concretely motivates the search for GNNs with higher expressive power than 2-WL or MPNN.
3. While a tight negative result for general k -WL is difficult to obtain, we show that T iterations of k -WL is unable to perform matching-count for the path pattern of $(k + 1)2^T$ or more nodes. It is relevant since real-life GNNs are often shallow, and also demonstrates an interplay between k and depth.

We complement these theoretical results with synthetic experiments of counting triangles and stars in random graphs. In addition, while our negative theoretical results are worst-case in nature, the experiments illustrate

an average-case difficulty for classical GNNs to count even the simplest graph substructures such as triangles. On the other hand, instead of performing iterative equivariant aggregations of information as is done in MPNNs and IGNNs, we propose a type of locally powerful models based on the intuition that substructures present themselves in local neighborhoods known as *egonets*. One idea is to apply the Relational Pooling approach (Murphy et al., 2019) to *egonets*, resulting in a model we call *Local Relational Pooling*. We demonstrate that it can perform both matching- and containment-count in the experiments.

2 Framework

2.1 Attributed graphs, (induced) subgraphs and two types of counting

An *unattributed graph* G with n nodes is usually denoted by $G = (V, E)$, where typically $V = [n] := \{1, \dots, n\}$ is the vertex set and $E \subset V^2 := V \times V$ is the edge set. We define an *attributed graph* or *weighted graph* as $G = (V, E, x, e)$, where in addition to V and E , we let $x_i \in \mathcal{X}$ represent the node feature of node i , and $e_{i,j} \in \mathcal{Y}$ represent the edge feature of edge (i, j) if $(i, j) \in E$. For simplicity, we consider undirected graphs (i.e. if $(i, j) \in E$ then $(j, i) \in E$ and $e_{i,j} = e_{j,i}$), and we do not allow self-connections (i.e., $(i, i) \notin E$) or multi-edges (so that E is a well-defined set). The graph can be equivalently represented by an adjacency matrix A together with the node and edge features. Two attributed graphs $G^{[1]} = (V^{[1]}, E^{[1]}, x^{[1]}, e^{[1]})$ and $G^{[2]} = (V^{[2]}, E^{[2]}, x^{[2]}, e^{[2]})$ are isomorphic if there exists a bijection $\pi : V^{[1]} \rightarrow V^{[2]}$ such that (1) $(i, j) \in E^{[1]}$ if and only if $(\pi(i), \pi(j)) \in E^{[2]}$, (2) $x_i^{[1]} = x_{\pi(i)}^{[2]}$ for all i in $V^{[1]}$, and (3) $e_{i,j}^{[1]} = e_{\pi(i), \pi(j)}^{[2]}$ for all $(i, j) \in E^{[1]}$. Note that an unattributed graph can be viewed as an attributed graph with identical node and edge features. If a graph has only node features and not edge features, we can also represent it as $G = (V, E, x)$.

Before defining substructure counting, we first need to define *subgraphs* and *induced subgraphs*. For $G = (V, E, x, e)$, a *subgraph* of G is any graph $G^{[S]} = (V^{[S]}, E^{[S]}, x, e)$ with $V^{[S]} \subseteq V$ and $E^{[S]} \subseteq E$. An *induced subgraph* of G is any graph $G^{[S']} = (V^{[S']}, E^{[S']}, x, e)$ with $V^{[S']} \subseteq V$ and $E^{[S']} = E \cap (V^{[S']})^2$. In words, an induced subgraph needs to include all edges in E whose both end points belong to $V^{[S']}$ as its edges. Thus, an induced subgraph of G is also its subgraph, but the converse is not true.

We now define two types of counting attributed substructures: *matching* and *containment*, illustrated in Figure 1. Let $G^{[P]} = (V^{[P]}, E^{[P]}, x^{[P]}, e^{[P]})$ be a (typically smaller) graph that we refer to as a *pattern* or *substructure*. We define $C(G, G^{[P]})$, called the *containment-count* of $G^{[P]}$ in G , to be the number of *subgraphs* of G that are isomorphic to $G^{[P]}$. We define $M(G, G^{[P]})$, called the *matching-count* of $G^{[P]}$ in G , to be the number of *induced subgraphs* of G that are isomorphic to $G^{[P]}$. Since all induced subgraphs are subgraphs, we always have $M(G, G^{[P]}) \leq C(G, G^{[P]})$.

Moreover, on a space of graphs \mathcal{G} , we call $M(\cdot; G^{[P]})$ the *matching-count function* of the pattern $G^{[P]}$, and $C(\cdot; G^{[P]})$ the *containment-count function* of $G^{[P]}$. To formalize the question whether certain GNN architectures can count different substructures, a natural object to study is their ability to *approximate the matching-count and the containment-count functions arbitrarily well*. Formally, given a target function $g : \mathcal{G} \rightarrow \mathbb{R}$, and family of functions, \mathcal{F} , which in our case is typically the family of functions that a GNN architecture can represent, we say \mathcal{F} is able to approximate g on \mathcal{G} if for all $\epsilon > 0$ there exists $f \in \mathcal{F}$ such that $|g(G) - f(G)| < \epsilon$, for all $G \in \mathcal{G}$.

However, such criterion based on function approximation is hard to work with directly when we look at concrete examples later on. For this reason, below we will look for an alternative and equivalent definition from the perspective of graph discrimination.

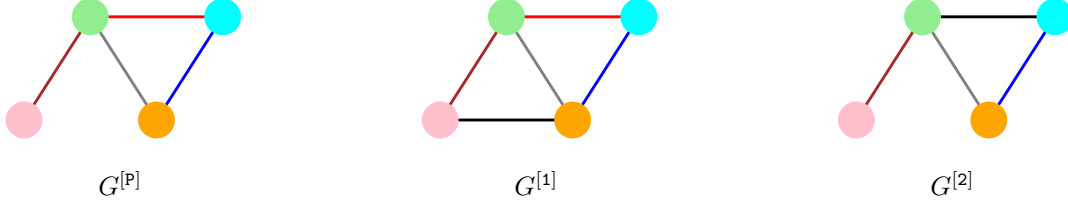


Figure 1: Illustration of containment-count and matching-count. Consider the graphs $G^{[P]}$, $G^{[1]}$, $G^{[2]}$ where the edge and node features are represented by colors. The matching-count $M(G^{[1]}; G^{[P]}) = 0$ but the containment-count $C(G^{[1]}; G^{[P]}) = 1$, whereas $M(G^{[2]}; G^{[P]}) = C(G^{[2]}; G^{[P]}) = 0$ because the edge features do not match.

2.2 From function approximation to graph discrimination

Say \mathcal{G} is a space of graphs, and \mathcal{F} is a family of functions from \mathcal{G} to \mathbb{R} . Given two graphs $G^{[1]}, G^{[2]} \in \mathcal{G}$, we say \mathcal{F} is able to distinguish them if there exists $f \in \mathcal{F}$ such that $f(G^{[1]}) \neq f(G^{[2]})$. Such a perspective has been explored in [Chen et al. \(2019b\)](#), for instance, to build an equivalence between function approximation and graph isomorphism testing by GNNs. In the context of substructure counting, it is clear that the ability to approximate the count functions entails the ability to distinguish graphs in the following sense:

Observation 1. *If \mathcal{F} is able to approximate the matching-count (or containment-count) function of a pattern $G^{[P]}$ on the space \mathcal{G} , then for all $G^{[1]}, G^{[2]} \in \mathcal{G}$ such that $M(G^{[1]}, G^{[P]}) \neq M(G^{[2]}, G^{[P]})$ (or $C(G^{[1]}, G^{[P]}) \neq C(G^{[2]}, G^{[P]})$), they can be distinguished by \mathcal{F} .*

What about the converse? When the space \mathcal{G} is finite, such as if the graphs have bounded numbers of nodes and the node as well as edge features belong to finite alphabets, we can show a slightly weaker statement than the exact converse. Following [Chen et al. \(2019b\)](#), we define an augmentation of families of functions using feed-forward neural networks as follows:

Definition 1. *Given \mathcal{F} , a family of functions from a space \mathcal{X} to \mathbb{R} , we consider an augmented family of functions also from \mathcal{X} to \mathbb{R} consisting of all functions of the following form*

$$x \mapsto h_{\mathcal{NN}}([f_1(x), \dots, f_d(x)]),$$

where $d \in \mathbb{N}$, $h_1, \dots, h_d \in \mathcal{F}$, and $h_{\mathcal{NN}}$ is a feed-forward neural network / multi-layer perceptron. When \mathcal{NN} is restricted to have L layers at most, we denote this augmented family by \mathcal{F}^{+L} .

Lemma 1. *Suppose \mathcal{X} is a finite space, g is a finite function on \mathcal{X} , and \mathcal{F} is a family of functions on \mathcal{X} . Then, \mathcal{F}^{+1} is able to approximate g on \mathcal{G} if $\forall x_1, x_2 \in \mathcal{X}$ with $g(x_1) \neq g(x_2)$, $\exists f \in \mathcal{F}$ such that $f(x_1) \neq f(x_2)$.*

Proof. Since \mathcal{X} is a finite space, for some large enough integer d , \exists a collection of d functions, $f_1, \dots, f_d \in \mathcal{F}$ such that, if we define the function $\mathbf{f}(x) = (f_1(x), \dots, f_d(x)) \in \mathbb{R}^d$, then it holds that $\forall x_1, x_2 \in \mathcal{X}, \mathbf{f}(x_1) = \mathbf{f}(x_2) \Rightarrow g(x_1) = g(x_2)$. (In fact, we can choose $d \leq \frac{|\mathcal{X}| \cdot (|\mathcal{X}| - 1)}{2}$, since in the worst case we need one f_i per pair of $x_1, x_2 \in \mathcal{X}$ with $x_1 \neq x_2$.) Then, \exists a well-defined function h from \mathbb{R}^d to \mathbb{R} such that $\forall x \in \mathcal{X}, g(x) = h(\mathbf{f}(x))$. By the universal approximation power of neural networks, h can then be approximated arbitrarily well by some neural network $h_{\mathcal{NN}}$. \square

Thus, in the context of substructure counting, we have the following observation.

Observation 2. *Suppose \mathcal{G} is a finite space. If $\forall G^{[1]}, G^{[2]} \in \mathcal{G}$ with $M(G^{[1]}, G^{[P]}) \neq M(G^{[2]}, G^{[P]})$ (or $C(G^{[1]}, G^{[P]}) \neq C(G^{[2]}, G^{[P]})$), \mathcal{F} is able to distinguish $G^{[1]}$ and $G^{[2]}$, then \mathcal{F}^{+1} is able to approximate the matching-count (or containment-count) function of the pattern $G^{[P]}$ on \mathcal{G} .*

For many GNN families, \mathcal{F}^{+1} in fact has the same expressive power as \mathcal{F} . For example, consider $\mathcal{F}_{\text{MPNN}}$, the family of all Message Passing Neural Networks on \mathcal{G} . $\mathcal{F}_{\text{MPNN}}^{+1}$ consists of functions that run several MPNNs on the input graph in parallel and stack their outputs to pass through an MLP. However, running several MPNNs in parallel is equivalent to running one MPNN with larger dimensions of hidden states and messages, and moreover the additional MLP at the end can be merged into the readout function. Similar holds for the family of all k -Invariant Graph Functions (k -IGNs). Hence, for such GNN families, we have an exact equivalence on finite graph spaces \mathcal{G} .

Therefore, we define substructure counting alternatively as follows, which are equivalent thanks to the results above and easier to work with when we study particular GNN architectures:

Definition 2. We say \mathcal{F} is able to perform matching-count (or containment-count) of a pattern $G^{[p]}$ on \mathcal{G} if $\forall G^{[1]}, G^{[2]} \in \mathcal{G}$ such that $M(G^{[1]}, G^{[p]}) \neq M(G^{[2]}, G^{[p]})$ (or $C(G^{[1]}, G^{[p]}) \neq C(G^{[2]}, G^{[p]})$), \mathcal{F} is able to distinguish $G^{[1]}$ and $G^{[2]}$.

Another benefit of this definition is that it naturally allows us to also define the ability of graph isomorphism tests to count substructures. A graph isomorphism test, such as the Weisfeiler-Lehman (WL) test, takes as input a pair of graphs and returns whether or not they are believed to be isomorphic. Typically, the test will return true if the two graphs are indeed isomorphic but does not necessarily return false for every pair of non-isomorphic graphs. Given such a graph isomorphism test, we say it is able to perform matching-count (or containment-count) of a pattern $G^{[p]}$ on \mathcal{G} if $\forall G^{[1]}, G^{[2]} \in \mathcal{G}$ such that $M(G^{[1]}, G^{[p]}) \neq M(G^{[2]}, G^{[p]})$ (or $C(G^{[1]}, G^{[p]}) \neq C(G^{[2]}, G^{[p]})$), the test can tell these two graphs apart.

Additional notations used in the proofs are given in Appendix A.

3 Message Passing Neural Networks and the Weisfeiler-Lehman hierarchy

Message Passing Neural Network (MPNN) is a generic model that incorporates many popular architectures (Gilmer et al., 2017). When applied to an undirected graph $G = (V, E, x, e)$, an MPNN with T layers is defined iteratively as follows. For $t < T$, to compute the message $m_i^{(t+1)}$ and the hidden state $h_i^{(t+1)}$ for each node $i \in V$ at the $(t+1)$ th layer, we apply the following update rule:

$$\begin{aligned} m_i^{(t+1)} &= \sum_{\mathcal{N}(i)} M_t(h_i^{(t)}, h_j^{(t)}, e_{i,j}) \\ h_i^{(t+1)} &= U_t(h_i^{(t)}, m_i^{(t+1)}) \end{aligned}$$

where $\mathcal{N}(i)$ is the neighborhood of node i in G , M_t is the message function at layer t and U_t is the vertex update function at layer t . Finally, a graph-level prediction is computed as

$$\hat{y} = R(\{h_i^{(T)} : i \in V\}),$$

where R is the readout function. Typically, the hidden states at the first layer are set as $h_i^{(0)} = x_i$.

Xu et al. (2018a) and Morris et al. (2019) show that, when the graphs' edges are unweighted, such models are at most as powerful as the Weisfeiler-Lehman (WL) test, to be introduced below, in distinguishing non-isomorphic graphs. We will extend this result to incorporate edge features, which MPNNs naturally accommodate, so that by examining the ability of WL to count substructures, we can draw conclusions for MPNNs.

3.1 The hierarchy of k -Weisfeiler-Lehman tests

We will introduce the general k -WL test for $k \in \mathbb{N}^*$ applied to a pair of graphs, $G^{[1]}$ and $G^{[2]}$. Assume that the two graphs have the same number of vertices, since otherwise they can be told apart easily. Without loss of generality, we assume that they share the same set of vertex indices, V (but can differ in E , x or e). For each of the graphs, at iteration 0, the test assigns an initial color in some color space to every k -tuple in V^k according to its isomorphism type¹, and then updates the coloring in every iteration. For any k -tuple $s = (i_1, \dots, i_k) \in V^k$, we let $\mathbf{c}_k^{(t)}(s)$ denote the color of s in $G^{[1]}$ assigned at t th iteration, and let $\mathbf{c}'_k^{(t)}(s)$ denote the color it receives in $G^{[2]}$. $\mathbf{c}_k^{(t)}(s)$ and $\mathbf{c}'_k^{(t)}(s)$ are updated iteratively as follows. For each $w \in [k]$, define the neighborhood

$$N_w(s) = \{(i_1, \dots, i_{w-1}, j, i_{w+1}, \dots, i_k) : j \in V\}$$

Given $\mathbf{c}_k^{(t-1)}$ and $\mathbf{c}'_k^{(t-1)}$, define

$$\begin{aligned} C_w^{(t)}(s) &= \text{HASH}_{t,1} \left(\{ \mathbf{c}_k^{(t-1)}(\tilde{s}) : \tilde{s} \in N_w(s) \} \right) \\ C'_w{}^{(t)}(s) &= \text{HASH}_{t,1} \left(\{ \mathbf{c}'_k^{(t-1)}(\tilde{s}) : \tilde{s} \in N_w(s) \} \right) \end{aligned}$$

with “ $\{\}$ ” representing a multiset, and $\text{HASH}_{t,1}$ being some hash function that maps injectively from the space of multisets of colors to some intermediate space. Then let

$$\begin{aligned} \mathbf{c}_k^{(t)}(s) &= \text{HASH}_{t,2} \left(\left(\mathbf{c}_k^{(t-1)}(s), \left(C_1^{(t)}(s), \dots, C_k^{(t)}(s) \right) \right) \right) \\ \mathbf{c}'_k{}^{(t)}(s) &= \text{HASH}_{t,2} \left(\left(\mathbf{c}'_k^{(t-1)}(s), \left(C'_1{}^{(t)}(s), \dots, C'_k{}^{(t)}(s) \right) \right) \right) \end{aligned}$$

where $\text{HASH}_{t,2}$ maps injectively from its input space to the space of colors. The test will terminate and return the result that the two graphs are not isomorphic if at some iteration t , the following two multisets differ:

$$\{ \mathbf{c}_k^{(t)}(s) : s \in V^k \} \neq \{ \mathbf{c}'_k{}^{(t)}(s) : s \in V^k \}$$

Some properties of k -WL For graphs with unweighted edges, 1-WL and 2-WL are known to have the same discriminative power (Maron et al., 2019b). For $k \geq 2$, it is known that $(k+1)$ -WL is strictly more powerful than k -WL, in the sense that there exist pairs of graph distinguishable by the former but not the latter (Cai et al., 1992). Thus, with growing k , the set of k -WL tests forms a hierarchy with increasing discriminative power. Note that there has been an different definition of WL in the literature, sometimes known as *Folklore Weisfeiler-Lehman* (FWL), with different properties (Maron et al., 2019b; Morris et al., 2019). When people use the term “Weisfeiler-Lehman test” without specifying “ k ”, it usually refers to 1-WL, 2-WL or 1-FWL.

Extending the aforementioned results by Xu et al. (2018a); Morris et al. (2019) in a nontrivial way to incorporate edge features, we prove the following theorem in Appendix C.

Theorem 1. *Say two graphs $G^{[1]}$ and $G^{[2]}$ cannot be distinguished by 2-WL. Then there is no MPNN that can distinguish them.*

Proof intuition: If 2-WL cannot distinguish the two graphs, then at any iteration t , $\{ \mathbf{c}_k^{(t)}(s) : s \in V^2 \} = \{ \mathbf{c}'_k{}^{(t)}(s) : s \in V^2 \}$. This guarantees the existence of a bijective map from pairs of nodes in $G^{[1]}$ to pairs of nodes in $G^{[2]}$ that preserve the coloring. Through examining the update rules of 2-WL and MPNNs, we will show by induction that for any MPNN, at the t th layer, such a map will also preserve the hidden states of the nodes involved in the pair as well as the edge feature. This implies that any MPNN with t layers will

¹We define isomorphism types rigorously in Appendix B.

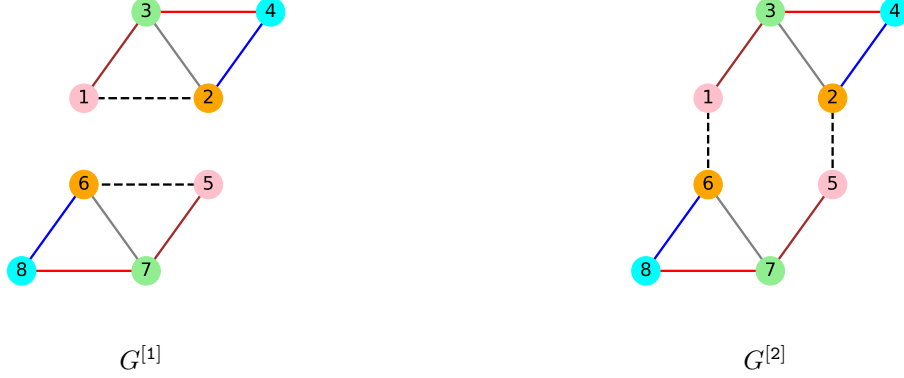


Figure 2: Illustration of the construction in the proof of Theorem 2 for the pattern from Figure 1 (left). Note that $M(G^{[1]}; G^{[P]}) = 0$ whereas $M(G^{[2]}; G^{[P]}) = 2$. The graphs $G^{[1]}$ and $G^{[2]}$ are not distinguishable by MPNNs, 2-WL, or 2-IGNs.

return identical outputs when applied to the two graphs.

This result motivates us to study what patterns 2-WL can and cannot count in the next subsection.

3.2 Substructure counting by 2-WL and MPNNs

For matching-count, we find a clear criterion based on the number of nodes in the pattern. Any connected pattern with 1 or 2 nodes (i.e., representing a node or an edge) can be easily counted by an MPNN with 0 or 1 layer of message-passing, respectively. On the other hand, we have the following theorem, to be proved in Appendix D.

Theorem 2. *2-WL cannot perform matching-count of any connected pattern with 3 or more nodes.*

Proof Intuition. Given any connected pattern of at least 3 nodes, we can construct a pair of graphs that have different matching-counts of the pattern but cannot be distinguished from each other by 2-WL. For instance, if we run 2-WL on the pair of graphs in Figure 2, then there will be $c_2^{(t)}((1, 3)) = c_2'^{(t)}((1, 3))$, $c_2^{(t)}((1, 2)) = c_2'^{(t)}((1, 6))$, $c_2^{(t)}((1, 6)) = c_2'^{(t)}((1, 2))$, and so on. We can in fact show that $\{c_2^{(t)}(s) : s \in V^2\} = \{c_2'^{(t)}(s) : s \in V^2\}$, $\forall t$.

Thus, together with Theorem 1, we have

Corollary 1. *MPNNs cannot perform matching-count of any connected pattern with 3 or more nodes.*

For containment-count, if both nodes and edges are unweighted, Arvind et al. (2018) show that the only patterns 1-WL (and equivalently 2-WL) can count are either star-shaped patterns and pairs of disjoint edges. We prove the positive result that MPNNs can count star-shaped patterns even when node and edge features are allowed, utilizing a result in Xu et al. (2018a) that the message functions are able to approximate any function on multisets.

Theorem 3. *MPNNs can perform containment-count of star-shaped patterns.*

By Theorem 1, this implies that

Corollary 2. *2-WL can perform containment-count of star-shaped patterns.*

3.3 Substructure counting by k -WL

There have been efforts to extend the power of GNNs by going after k -WL for higher k , such as [Morris et al. \(2019\)](#). Thus, it is also interesting to study the patterns that k -WL can and cannot count. Firstly, since k -tuples are assigned initial colors based on their isomorphism types, the following is easily seen, and we provide a proof in [Appendix F](#).

Theorem 4. *k -WL, at initialization, is able to perform both matching-count and containment-count of patterns consisting of at most k nodes.*

This establishes a potential hierarchy of increasing power in terms of substructure counting by k -WL. However, tighter results can be much harder to achieve. For example, to show that 2-FWL (and therefore 3-WL) cannot count cycles of length 8, [Fürer \(2017\)](#) has to rely on performing computer counting on the classical Cai-Fürer-Immerman counterexamples to k -WL ([Cai et al., 1992](#)). We leave the pursuit of general and tighter characterizations of k -WL’s substructure counting power for future research, but we are nevertheless able to provide a partial negative result concerning finite iterations of k -WL.

Definition 3. *A path pattern of size m , denoted by H_m , is an unattributed graph, $H_m = (V^{[H_m]}, E^{[H_m]})$, where $V^{[H_m]} = [m]$, and $E^{[H_m]} = \{(i, i+1) : 1 \leq i < m\} \cup \{(i+1, i) : 1 \leq i < m\}$.*

Theorem 5. *Running T iterations of k -WL cannot perform matching-count of any path pattern of $(k+1)2^T$ or more nodes.*

The proof is given in [Appendix G](#). This bound grows quickly when T becomes large. However, since in practice, many if not most GNN models are designed to be shallow ([Zhou et al., 2018](#); [Wu et al., 2019](#)), we believe this result is still relevant for studying finite-depth GNNs that are based on k -WL.

4 Invariant Graph Networks

Recently, an alternative hierarchy for GNNs was introduced in [Maron et al. \(2018\)](#) with universal approximation. We extend the negative results of the previous section by establishing an equivalence between IGNs and WL.

Definition 4. *A k th-order Invariant Graph Network (k -IGN) is a function $F : \mathbb{R}^{n^k \times d_0} \rightarrow \mathbb{R}$ that can be decomposed in the following way:*

$$F = m \circ h \circ L^{(T)} \circ \sigma \circ \dots \circ \sigma \circ L^{(1)},$$

where each $L^{(t)}$ is a linear equivariant layer from $\mathbb{R}^{n^k \times d_{t-1}}$ to $\mathbb{R}^{n^k \times d_t}$, σ is a pointwise activation function, h is a linear invariant layer from $\mathbb{R}^{n^k \times d_T}$ to \mathbb{R} , and m is an MLP.

A particularly interesting case is $k = 2$, partly because as k grows, the computational complexity in both space and time grows quickly, and the implementation becomes more complicated as well. Given a graph $G = (V = [n], E, x, e)$, supposing without loss of generality that the node and edge features both have dimension d , a 2-IGN takes as input a third-order tensor, $\mathbf{B}^{(0)} \in \mathbb{R}^{n \times n \times (d+1)}$, constructed in the following way: $\forall i \in [n], \mathbf{B}_{i,i,2:(d+1)}^{(0)} = x_i; \forall i, j \in [n]$ with $i \neq j$, $\mathbf{B}_{i,j,1}^{(0)} = A_{i,j}$ and $\mathbf{B}_{i,j,2:(d+1)}^{(0)} = e_{i,j}$. If we use $\mathbf{B}^{(t)}$ to denote the output of the t th layer of the 2-IGN, then they are defined iteratively by

$$\mathbf{B}^{(t+1)} = \sigma(L^{(t)}(\mathbf{B}^{(t)})) \quad (1)$$

4.1 2-IGNs equivalent to 2-WL

Before studying how well can 2-IGNs count substructures, we first relate it to 2-WL. It is known that 2-IGNs are at least as powerful as 2-WL, while the other direction remains an open problem ([Maron et al., 2019c,a](#)). Here we answer the question by proving the converse, that 2-IGNs are no more powerful than 2-WL. The full argument can be found in [Appendix H](#).

Theorem 6. *If two graphs $G^{[1]}$ and $G^{[2]}$ cannot be distinguished by the 2-WL test, then there is no 2-IGN that can distinguish them either.*

Proof intuition: Given a pair of nodes $(i, j) \in V^2$ with $i \neq j$, we can partition V^2 as the union of nine disjoint subsets: $\mathcal{A}_1 = \{(i, j)\}$, $\mathcal{A}_2 = \{(i, i)\}$, $\mathcal{A}_3 = \{(j, j)\}$, $\mathcal{A}_4 = \{(i, k) : k \neq i \text{ or } j\}$, $\mathcal{A}_5 = \{(k, i) : k \neq i \text{ or } j\}$, $\mathcal{A}_6 = \{(j, k) : k \neq i \text{ or } j\}$, $\mathcal{A}_7 = \{(k, j) : k \neq i \text{ or } j\}$, $\mathcal{A}_8 = \{(k, l) : k \neq l \text{ and } \{k, l\} \cap \{i, j\} = \emptyset\}$, and $\mathcal{A}_9 = \{(k, k) : k \notin \{i, j\}\}$. If 2-WL cannot distinguish the two graphs in t iterations, then there exists not only a color-preserving bijective map from pairs of nodes in $G^{[1]}$ to pairs of nodes in $G^{[2]}$, mapping (i, j) to some (i', j') , but also a color-preserving bijective map from \mathcal{A}_w to \mathcal{A}'_w for each $w \in [9]$, where \mathcal{A}'_w is the corresponding subset of V^2 associated with (i', j') . By the update rule of 2-IGNs, this allows us to show that $\mathbf{B}_{i,j}^{(t)} = \mathbf{B}_{i',j'}^{(t)}$, and hence a 2-IGN with t layers cannot return distinct outputs when applied to the two graphs.

Corollary 3. *2-IGNs are exactly as powerful as 2-WL.*

4.2 Substructure counting by 2-IGNs

Thanks to the equivalence shown above, the two following theorems are direct consequences of Theorem 2 and Corollary 2, though we also provide a direct proof of Corollary 4 in Appendix I.

Corollary 4. *2-IGNs cannot perform matching-count of any connected pattern with 3 or more nodes.*

Corollary 5. *2-IGNs can perform containment-count of star-shaped patterns.*

4.3 Substructure counting by k -IGNs

Maron et al. (2019b) prove that k -IGNs are no less powerful than k -WL. Thus, as a corollary of Theorem 4, we have

Theorem 7. *k -IGNs can perform both matching-count and containment-count of patterns consisting of at most k nodes.*

5 Local Relational Pooling

Though MPNNs and 2-IGNs are able to aggregate information from multi-hop neighborhoods, we have seen above that they are unable to preserve information such as the matching-counts of nontrivial patterns. To bypass such limitations, we suggest going beyond the strategy of iteratively aggregating information in an equivariant way, which underlies both MPNNs and IGNs. One helpful observation is that, if a pattern is present in the graph, it can always be found in a sufficiently large local neighborhood, or *egonet*, of some node in the graph (Preciado et al., 2012). An egonet of depth l centered at a node i is the induced subgraph consisting of i and all nodes within distance l from it. Note that any pattern with radius r is a subgraph of some egonet of depth $l = r$. Hence, by applying a powerful local model to each egonet separately and then aggregating the outputs, we could potentially obtain a model capable of counting patterns.

For such a local model, we adopt the Relational Pooling (RP) idea from Murphy et al. (2019). In summary, it creates a powerful permutation-invariant model by symmetrizing a powerful model that is not necessarily permutation-invariant, where the symmetrization is performed by averaging or summing over all permutations of the nodes' ordering. Formally, if $\mathbf{B} \in \mathbb{R}^{n \times n \times d}$ is a node-ordering-dependent representation of the graph G , such as the adjacency matrix or the $\mathbf{B}^{(0)}$ defined above for 2-IGNs, then define

$$f_{\text{RP}}(G) = \sum_{\pi \in S_n} \bar{f}(\pi \circ \mathbf{B}),$$

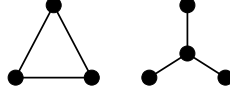


Figure 3: Substructures to be counted in the experiments. *Left*: A triangle. *Right*: A 3-star.

where \bar{f} can be some non-permutation-invariant function, S_n is the set of permutations on n nodes, and $\pi \circ \mathbf{B}$ is \mathbf{B} transformed by permuting its first two dimensions according to π . Such f 's are shown to be an universal approximators of permutation-invariant functions (Murphy et al., 2019). The summation quickly becomes intractable once n is large, and hence approximation methods have been introduced. In our case, however, since we apply this model to egonets that are usually smaller than the entire graph, the tractability issue is greatly alleviated. Moreover, since egonets are rooted graphs, we can reduce the symmetrization over all permutations in S_n to the subset $S_n^{\text{BFS}} \subseteq S_n$ of permutations compatible with breath-first-search (BFS) to further reduce the complexity, as suggested in Murphy et al. (2019).

Concretely, we define $G_{i,l}^{[\text{ego}]}$ as the egonet centered at node i of depth l , $\mathbf{B}_{i,l}^{[\text{ego}]}$ as the corresponding representation and $n_{i,l}$ as the number of nodes in $G_{i,l}^{[\text{ego}]}$. For computational efficiency, every tensor representation of egonet \mathbf{B} is cropped into a fixed-sized subtensor $C_k(\mathbf{B}) = \mathbf{B}_{[k],[k],:} \in \mathbb{R}^{k \times k \times d}$. Then our model over the entire graph G is expressed as

$$f_{\text{LRP}}^{l,k}(G) = \sum_{i \in V} \sum_{\pi \in S_{n_{i,l}}^{\text{BFS}}} \bar{f} \left(C_k(\pi \circ \mathbf{B}_{i,l}^{[\text{ego}]}) \right)$$

We call it depth- l size- k *Local Relational Pooling* (LRP- l - k). If node degrees are upper-bounded by D , the time complexity is $O(n \cdot (D!)^{D^l} \cdot k^2)$, and hence linear in n if D, k and l are fixed. In the experiments below, we implement a variant of LRP-1-4 designed as, with bias terms ignored,

$$\tilde{f}_{\text{LRP}}^{1,4}(G) = \mathbf{W}_1 \sum_{i \in V} \sigma \left[\frac{\text{MLP}(D_i)}{|S_{n_{i,1}}^{\text{BFS}}|} \odot \sum_{\pi \in S_{n_{i,1}}^{\text{BFS}}} f_*(\pi \circ \mathbf{B}_{i,1}^{[\text{ego}]}) \right],$$

where D_i is the degree of node i , σ is ReLU, MLP maps from \mathbb{R} to \mathbb{R}^H , where H is the hidden dimension, $\mathbf{W}_1 \in \mathbb{R}^{1 \times H}$ and $\forall j \in [H]$, $(f_*(\mathbf{X}))_j = \tanh(\sum \mathbf{W}_{2,j} \odot C_4(\mathbf{X})) \in \mathbb{R}$ with $\mathbf{W}_{2,j} \in \mathbb{R}^{4 \times 4 \times d}$. The motivation of $\text{MLP}(D_i)$ is to adaptively learn an invariant function over permutation, such as summing and averaging.

6 Experiments

Tasks. In this section, we verify our theoretical results on two graph-level regression tasks: *matching-counting triangles* and *containment-counting 3-stars*, with both patterns unattributed, as illustrated in Figure 3. By Theorem 2 and Corollary 1, MPNNs and 2-IGNs can perform matching-count of triangles. Note that since a triangle is a clique, its matching-count and containment-count are equal. We generate the ground-truth counts of triangles in each graph with an counting algorithm proposed by Shervashidze et al. (2009). By Theorem 3 and Corollary 2, MPNNs and 2-IGNs can perform containment-count though not matching-count of 3-stars. For its ground-truth count, we compute the number of stars centered at each node as $\binom{d}{3}$, where d is the degree of each node, and then sum over all nodes in the graph.

Synthetic datasets. We generate two synthetic datasets of random unattributed graphs. The first one is a set of 5000 Erdős-Renyi random graphs denoted as $ER(m, p)$, where $m = 10$ is the number of nodes

in each graph and $p = 0.3$ is the probability that an edge exists. The second one is a set of 5000 random regular graphs (Steger and Wormald, 1999) denoted as $RG(m, d)$, where m is the number of nodes in each graph and d is the node degree. We uniformly sample (m, d) from $\{(10, 6), (15, 6), (20, 5), (30, 5)\}$. We also randomly delete m edges in each graph from the second dataset. For both datasets, we randomly split them into training-validation-test sets with percentages 30%-20%-50%.

Models. We consider LRP, GIN (Xu et al., 2018a), GCN (Kipf and Welling, 2016), 2-IGN (Maron et al., 2018) and spectral GNN (sGNN) (Chen et al., 2019a), with GIN and GCN belonging to the category of MPNNs. Details of GNN architectures are provided in Appendix J. We use mean squared error (MSE) for regression loss. Each model is trained on 1080ti five times with different random seeds.

Results. The test loss of the two tasks are shown in Table 1. The bottom column shows the variance of the ground-truth counts of the pattern computed over all graphs in the dataset, which acts as a naive baseline. Compared to this baseline and the other models, the almost-negligible error of LRP supports our theory that depth-1 LRP is powerful enough for counting triangles and 3-stars, both of which have radius 1. GIN, 2-IGN and sGNN produce much smaller test error than the count variance for the containment-count of 3-star tasks, consistent with their theoretical power to containment-count stars. Relative to the count-variance baseline, GIN and 2-IGN have worse top performance on the triangle task than on the 3-star task, also as expected from the theory. However, the experiment results provide interesting insights into the average-case performance in the substructure counting tasks, which are beyond what our theory can predict at this point.

Table 1: Test MSE of different GNNs for matching-counting triangles and containment-counting 3-stars on the two datasets. Shown here are the best and median performance of one model over five runs. For each of GCN, GIN and sGNN, the best out of its four variants are selected. Details of the GNN architectures and raw results can be found in Appendices J, K.

	Erdős-Renyi				Random Regular			
	Triangle (M)		3-Star (C)		Triangle (M)		3-Star (C)	
	top 1	top 3	top 1	top 3	top 1	top 3	top 1	top 3
LRP-1-4	0.00115	0.00183	0.00674	0.0163	0.00233	0.00361	0.000594	0.000889
2-IGN	0.890	1.70	0.168	15.9	2.47	5.614	19.3	302
GIN	0.905	0.920	0.0505	0.107	4.43	4.47	0.118	0.147
GCN	4.98	6.07	136	142	17.2	19.4	832	885
sGNN	0.680	0.827	0.736	2.40	3.70	4.17	7.50	44.5
<i>count var.</i>	7.34		311.2		9.42		316.1	

7 Conclusions

We propose a theoretical framework to study the expressive power of classes of GNNs based on their ability to count substructures. We distinguish two kinds of counting: containment-count (counting subgraphs) and matching-count (counting induced subgraphs). We prove that neither MPNNs nor 2-IGNs can matching-count any connected structure with 3 or more nodes; k -IGNs and k -WL can containment-count and matching-count any pattern of size k . We also provide an upper bound on the size of “path-shaped” substructures that finite iterations of k -WL can matching-count. To establish these results, we prove an equivalence between approximating graph functions and discriminating graphs. Also, as intermediary results, we prove that MPNNs are no more powerful than 2-WL on attributed graphs, and that 2-IGNs are equivalent to 2-WL in distinguishing non-isomorphic graphs, which partly answers an open problem raised in Maron et al. (2019a). In addition, we perform numerical experiments that support our theoretical results and show that the Local

Relational Pooling approach inspired by [Murphy et al. \(2019\)](#) can successfully count certain substructures. In summary, we build the foundation for using substructure counting as an intuitive and relevant measure of the expressive power of GNNs, and our concrete results for existing GNNs motivate the search for more powerful designs of GNNs.

One limitation of our theory is that it only pertains to the expressive power of GNNs and does not speak about optimization or generalization. In addition, our theoretical results are worse-case in nature and cannot predict average-case performance, which is interesting to study as well. Nonetheless, even within this new framework, many interesting questions remain, including better characterizing the ability to count substructures of general k -WL and k -IGNs as well as other architectures such as spectral GNNs ([Chen et al., 2019a](#)) and polynomial IGNs ([Maron et al., 2019a](#)). Another interesting future direction is to study the relevance of substructure counting in empirical tasks, following the work of [Ying et al. \(2019\)](#).

Acknowledgements We would like to thank Haggai Maron and Jiaxuan You for nice conversations. This work is partially supported by the Alfred P. Sloan Foundation, NSF RI-1816753, NSF CAREER CIF 1845360, NSF CHS-1901091, Samsung Electronics, and the Institute for Advanced Study. SV is partly supported by NSF DMS 1913134, EOARD FA9550-18-1-7007 and the Simons Algorithms and Geometry (A&G) Think Tank.

References

- Alon, N., Dao, P., Hajirasouliha, I., Hormozdiari, F., and Sahinalp, S. C. (2008). Biomolecular network motif counting and discovery by color coding. *Bioinformatics*, 24(13):i241–i249.
- Arvind, V., Fuhlbrück, F., Köbler, J., and Verbitsky, O. (2018). On weisfeiler-leman invariance: Subgraph counts and related graph properties. *arXiv preprint arXiv:1811.04801*.
- Babai, L., Erdos, P., and Selkow, S. M. (1980). Random graph isomorphism. *SIAM Journal on computing*, 9(3):628–635.
- Bronstein, M. M., Bruna, J., LeCun, Y., Szlam, A., and Vandergheynst, P. (2017). Geometric deep learning: Going beyond euclidean data. *IEEE Signal Processing Magazine*, 34(4):18–42.
- Bruna, J., Zaremba, W., Szlam, A., and LeCun, Y. (2013). Spectral networks and locally connected networks on graphs. *arXiv preprint arXiv:1312.6203*.
- Cai, J.-Y., Fürer, M., and Immerman, N. (1992). An optimal lower bound on the number of variables for graph identification. *Combinatorica*, 12(4):389–410.
- Chen, Z., Li, L., and Bruna, J. (2019a). Supervised community detection with line graph neural networks. *International Conference on Learning Representations*.
- Chen, Z., Villar, S., Chen, L., and Bruna, J. (2019b). On the equivalence between graph isomorphism testing and function approximation with gnns. In *Advances in Neural Information Processing Systems*, pages 15868–15876.
- Choma, N., Monti, F., Gerhardt, L., Palczewski, T., Ronaghi, Z., Prabhat, P., Bhimji, W., Bronstein, M., Klein, S., and Bruna, J. (2018). Graph neural networks for icecube signal classification. In *2018 17th IEEE International Conference on Machine Learning and Applications (ICMLA)*, pages 386–391. IEEE.
- Dai, H., Khalil, E. B., Zhang, Y., Dilkina, B., and Song, L. (2017). Learning combinatorial optimization algorithms over graphs. *arXiv preprint arXiv: 1704.01665*.

- Defferrard, M., Bresson, X., and Vandergheynst, P. (2016). Convolutional neural networks on graphs with fast localized spectral filtering. In *Advances in neural information processing systems*, pages 3844–3852.
- Deshpande, M., Kuramochi, M., and Karypis, G. (2002). Automated approaches for classifying structures. Technical report, Minnesota University Minneapolis Department of Computer Science.
- Ding, M., Zhou, C., Chen, Q., Yang, H., and Tang, J. (2019). Cognitive graph for multi-hop reading comprehension at scale. In *Proceedings of the 57th Annual Meeting of the Association for Computational Linguistics*, pages 2694–2703, Florence, Italy. Association for Computational Linguistics.
- Duvenaud, D. K., Maclaurin, D., Iparraguirre, J., Bombarell, R., Hirzel, T., Aspuru-Guzik, A., and Adams, R. P. (2015). Convolutional networks on graphs for learning molecular fingerprints. In *Advances in neural information processing systems*, pages 2224–2232.
- Fürer, M. (2017). On the combinatorial power of the Weisfeiler-Lehman algorithm. *arXiv preprint arXiv:1704.01023*.
- Gilmer, J., Schoenholz, S. S., Riley, P. F., Vinyals, O., and Dahl, G. E. (2017). Neural message passing for quantum chemistry. In *Proceedings of the 34th International Conference on Machine Learning-Volume 70*, pages 1263–1272. JMLR. org.
- Ioffe, S. and Szegedy, C. (2015). Batch normalization: Accelerating deep network training by reducing internal covariate shift. *arXiv preprint arXiv:1502.03167*.
- Jiang, C., Coenen, F., and Zito, M. (2010). Finding frequent subgraphs in longitudinal social network data using a weighted graph mining approach. In *International Conference on Advanced Data Mining and Applications*, pages 405–416. Springer.
- Jin, W., Barzilay, R., and Jaakkola, T. (2019). Hierarchical graph-to-graph translation for molecules.
- Jin, W., Barzilay, R., and Jaakkola, T. S. (2018). Junction tree variational autoencoder for molecular graph generation. *CoRR*, abs/1802.04364.
- Keriven, N. and Peyré, G. (2019). Universal invariant and equivariant graph neural networks. *arXiv preprint arXiv:1905.04943*.
- Kingma, D. P. and Ba, J. (2014). Adam: A method for stochastic optimization. *arXiv preprint arXiv:1412.6980*.
- Kipf, T. N. and Welling, M. (2016). Semi-supervised classification with graph convolutional networks. *arXiv preprint arXiv:1609.02907*.
- Koyutrk, M., Grama, A., and Szpankowski, W. (2004). An efficient algorithm for detecting frequent subgraphs in biological networks. *Bioinformatics*, 20(suppl 1):i200–i207.
- Lemke, T. L. (2003). *Review of organic functional groups: introduction to medicinal organic chemistry*. Lippincott Williams & Wilkins.
- Liu, S., Chandereng, T., and Liang, Y. (2018). N-gram graph, A novel molecule representation. *arXiv preprint arXiv:1806.09206*.
- Liu, X., Pan, H., He, M., Song, Y., and Jiang, X. (2019). Neural subgraph isomorphism counting.
- Loukas, A. (2019). What graph neural networks cannot learn: depth vs width. *arXiv preprint arXiv:1907.03199*.
- Maron, H., Ben-Hamu, H., and Lipman, Y. (2019a). Open problems: Approximation power of invariant graph networks.

- Maron, H., Ben-Hamu, H., Serviansky, H., and Lipman, Y. (2019b). Provably powerful graph networks. In *Advances in Neural Information Processing Systems*, pages 2153–2164.
- Maron, H., Ben-Hamu, H., Shamir, N., and Lipman, Y. (2018). Invariant and equivariant graph networks.
- Maron, H., Fetaya, E., Segol, N., and Lipman, Y. (2019c). On the universality of invariant networks. *arXiv preprint arXiv:1901.09342*.
- Monti, F., Otness, K., and Bronstein, M. M. (2018). Motifnet: a motif-based graph convolutional network for directed graphs. *CoRR*, abs/1802.01572.
- Morgan, H. L. (1965). The generation of a unique machine description for chemical structures—a technique developed at chemical abstracts service. *Journal of Chemical Documentation*, 5(2):107–113.
- Morris, C., Ritzert, M., Fey, M., Hamilton, W. L., Lenssen, J. E., Rattan, G., and Grohe, M. (2019). Weisfeiler and leman go neural: Higher-order graph neural networks. *Association for the Advancement of Artificial Intelligence*.
- Murphy, R. L., Srinivasan, B., Rao, V., and Ribeiro, B. (2019). Relational pooling for graph representations. *arXiv preprint arXiv:1903.02541*.
- Nowak, A., Villar, S., Bandeira, A. S., and Bruna, J. (2017). A note on learning algorithms for quadratic assignment with graph neural networks. *arXiv preprint arXiv:1706.07450*.
- OBoyle, N. M. and Sayle, R. A. (2016). Comparing structural fingerprints using a literature-based similarity benchmark. *Journal of cheminformatics*, 8(1):1–14.
- Preciado, V. M., Draief, M., and Jadbabaie, A. (2012). Structural analysis of viral spreading processes in social and communication networks using egonets.
- Rahman, S. A., Bashton, M., Holliday, G. L., Schrader, R., and Thornton, J. M. (2009). Small molecule subgraph detector (smsd) toolkit. *Journal of cheminformatics*, 1(1):12.
- Scarselli, F., Gori, M., Tsoi, A. C., Hagenbuchner, M., and Monfardini, G. (2008). The graph neural network model. *IEEE Transactions on Neural Networks*, 20(1):61–80.
- Shervashidze, N., Vishwanathan, S., Petri, T., Mehlhorn, K., and Borgwardt, K. (2009). Efficient graphlet kernels for large graph comparison. In *Artificial Intelligence and Statistics*, pages 488–495.
- Steger, A. and Wormald, N. C. (1999). Generating random regular graphs quickly. *Combinatorics, Probability and Computing*, 8(4):377–396.
- Weisfeiler, B. and Leman, A. (1968). The reduction of a graph to canonical form and the algebra which appears therein. *Nauchno-Technicheskaya Informatsia*, 2(9):12-16.
- Wu, Z., Pan, S., Chen, F., Long, G., Zhang, C., and Yu, P. S. (2019). A comprehensive survey on graph neural networks. *arXiv preprint arXiv:1901.00596*.
- Xu, K., Hu, W., Leskovec, J., and Jegelka, S. (2018a). How powerful are graph neural networks? *arXiv preprint arXiv:1810.00826*.
- Xu, K., Li, C., Tian, Y., Sonobe, T., Kawarabayashi, K.-i., and Jegelka, S. (2018b). Representation learning on graphs with jumping knowledge networks. *arXiv preprint arXiv:1806.03536*.
- Yao, W., Bandeira, A. S., and Villar, S. (2019). Experimental performance of graph neural networks on random instances of max-cut. In *Wavelets and Sparsity XVIII*, volume 11138, page 111380S. International Society for Optics and Photonics.

- Ying, R., Bourgeois, D., You, J., Zitnik, M., and Leskovec, J. (2019). Gnn explainer: A tool for post-hoc explanation of graph neural networks. *arXiv preprint arXiv:1903.03894*.
- Ying, R., You, J., Morris, C., Ren, X., Hamilton, W. L., and Leskovec, J. (2018). Hierarchical graph representation learning with differentiable pooling. *CoRR*, abs/1806.08804.
- You, J., Liu, B., Ying, Z., Pande, V., and Leskovec, J. (2018a). Graph convolutional policy network for goal-directed molecular graph generation. In *Advances in neural information processing systems*, pages 6410–6421.
- You, J., Ying, R., Ren, X., Hamilton, W. L., and Leskovec, J. (2018b). Graphrnn: A deep generative model for graphs. *CoRR*, abs/1802.08773.
- Zaheer, M., Kottur, S., Ravanbakhsh, S., Poczos, B., Salakhutdinov, R. R., and Smola, A. J. (2017). Deep sets. In *Advances in neural information processing systems*, pages 3391–3401.
- Zhang, M. and Chen, Y. (2018). Link prediction based on graph neural networks. In *Advances in Neural Information Processing Systems*, pages 5165–5175.
- Zhou, J., Cui, G., Zhang, Z., Yang, C., Liu, Z., Wang, L., Li, C., and Sun, M. (2018). Graph neural networks: A review of methods and applications. *arXiv preprint arXiv:1812.08434*.

A Additional notations

For two positive integers a and b , we define $\text{MOD}_a(b)$ to be a if a divides b and the number c such that $b \equiv c \pmod{a}$ otherwise. Hence the value ranges from 1 to a as we vary $b \in \mathbb{N}^*$.

For a positive integer c , let $[c]$ denote the set $\{1, \dots, c\}$.

Two k -types, $(i_1, \dots, i_k), (j_1, \dots, j_k) \in V^k$ are said to be in the same *equivalent class* if \exists a permutation π on V such that $(\pi(i_1), \dots, \pi(i_k)) = (j_1, \dots, j_k)$. Note that belonging to the same equivalence class is a weaker condition than having the same isomorphism type, as will be defined in Appendix B, which has to do with what the graphs look like.

For any k -tuple, $s = (i_1, \dots, i_k)$, and for $w \in [k]$, use $I_w(s)$ to denote the w th entry of s , i_w .

B Isomorphism types of k -tuples in k -WL for attributed graphs

Say $G^{[1]} = (V^{[1]}, E^{[1]}, x^{[1]}, e^{[1]})$, $G^{[2]} = (V^{[2]}, E^{[2]}, x^{[2]}, e^{[2]})$.

a) $\forall s = (i_1, \dots, i_k), s' = (i'_1, \dots, i'_k) \in (V^{[1]})^k$, s and s' are said to have the same isomorphism type if

1. $\forall \alpha, \beta \in [k], i_\alpha = i_\beta \Leftrightarrow i'_\alpha = i'_\beta$
2. $\forall \alpha \in [k], x_{i_\alpha}^{[1]} = x_{i'_\alpha}^{[1]}$
3. $\forall \alpha, \beta \in [k], (i_\alpha, i_\beta) \in E^{[1]} \Leftrightarrow (i'_\alpha, i'_\beta) \in E^{[1]}$, and moreover, if either side is true, then $e_{i_\alpha, i_\beta}^{[1]} = e_{i'_\alpha, i'_\beta}^{[1]}$

b) Similar if both $s, s' \in (V^{[2]})^k$.

c) $\forall s = (i_1, \dots, i_k) \in (V^{[1]})^k, s' = (i'_1, \dots, i'_k) \in (V^{[2]})^k$, s and s' are said to have the same isomorphism type if

1. $\forall \alpha, \beta \in [k], i_\alpha = i_\beta \Leftrightarrow i'_\alpha = i'_\beta$
2. $\forall \alpha \in [k], x_{i_\alpha}^{[1]} = x_{i'_\alpha}^{[2]}$
3. $\forall \alpha, \beta \in [k], (i_\alpha, i_\beta) \in E^{[1]} \Leftrightarrow (i'_\alpha, i'_\beta) \in E^{[2]}$, and moreover, if either side is true, then $e_{i_\alpha, i_\beta}^{[1]} = e_{i'_\alpha, i'_\beta}^{[2]}$

In k -WL tests, two k -tuples s and s' in either $(V^{[1]})^k$ or $(V^{[2]})^k$ are assigned the same color at iteration 0 if and only if they have the same isomorphism type.

For a reference, see [Maron et al. \(2019b\)](#).

C Proof of Theorem 1 (MPNNs are no more powerful than 2-WL)

Proof. Suppose for contradiction that there exists an MPNN with T_0 layers that can distinguish the two graphs. Let $m^{(t)}$ and $h^{(t)}$, $m'^{(t)}$ and $h'^{(t)}$ be the messages and hidden states at layer t obtained by applying the MPNN on the two graphs, respectively. Define

$$\tilde{h}_{i,j}^{(t)} = \begin{cases} h_i^{(t)} & \text{if } i = j \\ \left(h_i^{(t)}, h_j^{(t)}, a_{i,j}, e_{i,j} \right) & \text{otherwise} \end{cases}$$

$$\tilde{h}'_{i,j}^{(t)} = \begin{cases} h'_i{}^{(t)} & \text{if } i = j \\ \left(h'_i{}^{(t)}, h'_j{}^{(t)}, a'_{i,j}, e'_{i,j} \right) & \text{otherwise,} \end{cases}$$

where $a_{i,j} = 1$ if $(i,j) \in E^{[1]}$ and 0 otherwise, $e_{i,j} = e_{i,j}^{[1]}$ is the edge feature of the first graph, and a', e' are defined similarly for the second graph.

Since the two graphs cannot be distinguished by 2-WL, then for the T_0 th iteration, there is

$$\{\mathbf{c}_2^{(T_0)}(s) : s \in V^2\} = \{\mathbf{c}'_2^{(T_0)}(s) : s \in V^2\},$$

which implies that there exists a permutation on V^2 , which we can call η_0 , such that $\forall s \in V^2$, there is $\mathbf{c}_2^{(T_0)}(s) = \mathbf{c}'_2^{(T_0)}(\eta_0(s))$. To take advantage of this condition, we introduce the following lemma, which is central to the proof.

Lemma 2. $\forall t \leq T_0, \forall i, j, i', j' \in V$, if $\mathbf{c}_2^{(t)}((i, j)) = \mathbf{c}'_2^{(t)}((i', j'))$, then

1. $i = j \Leftrightarrow i' = j'$.
2. $\tilde{h}_{i,j}^{(t)} = \tilde{h}_{i',j'}^{(t)}$.

Proof of Lemma 2: First, we state the following simple observation without proof, which is immediate given the update rule of k -WL:

Lemma 3. For k -WL, $\forall s, s' \in V^k$, if for some t_0 , $\mathbf{c}_k^{(t_0)}(s) = \mathbf{c}'_k^{(t_0)}(s')$, then $\forall t \in [0, t_0]$, $\mathbf{c}_k^{(t)}(s) = \mathbf{c}'_k^{(t)}(s')$.

For the first condition, assuming $\mathbf{c}_2^{(t)}((i, j)) = \mathbf{c}'_2^{(t)}((i', j'))$, Lemma 3 then tells us that $\mathbf{c}_2^{(0)}((i, j)) = \mathbf{c}'_2^{(0)}((i', j'))$. Since the colors in 2-WL are initialized by the isomorphism type of the node pair, it has to be that $i = j \Leftrightarrow i' = j'$.

We will prove the second condition by induction on t . For the base case, $t = 0$, we want to show that $\forall i, j, i', j' \in V$, if $\mathbf{c}_2^{(0)}((i, j)) = \mathbf{c}'_2^{(0)}((i', j'))$ then $\tilde{h}_{i,j}^{(0)} = \tilde{h}_{i',j'}^{(0)}$. If $i = j$, then $\mathbf{c}_2^{(0)}((i, i)) = \mathbf{c}'_2^{(0)}((i', i'))$ if and only if $x_i = x_{i'}$, which is equivalent to $h_i^{(0)} = h_{i'}^{(0)}$, and hence $\tilde{h}_i^{(0)} = \tilde{h}_{i'}^{(0)}$. If $i \neq j$, then by the definition of isomorphism types given in Appendix B, $\mathbf{c}_2^{(0)}((i, j)) = \mathbf{c}'_2^{(0)}((i', j'))$ implies that

$$\begin{aligned} x_i &= x_{i'} \Rightarrow h_i^{(0)} = h_{i'}^{(0)} \\ x_j &= x_{j'} \Rightarrow h_j^{(0)} = h_{j'}^{(0)} \\ a_{i,j} &= a'_{i',j'} \\ e_{i,j} &= e'_{i',j'} \end{aligned}$$

which yields $\tilde{h}_{i,j}^{(0)} = \tilde{h}_{i',j'}^{(0)}$.

Next, to prove the inductive step, assume that for some $T \in [T_0]$, the statement in Lemma 2 holds for all $t \leq T - 1$, and consider $\forall i, j, i', j' \in V$ such that $\mathbf{c}_2^{(T)}((i, j)) = \mathbf{c}'_2^{(T)}((i', j'))$. By the update rule of 2-WL, this implies that

$$\begin{aligned} \mathbf{c}_2^{(T-1)}((i, j)) &= \mathbf{c}'_2^{(T-1)}((i', j')) \\ \{\mathbf{c}_2^{(T-1)}((k, j)) : k \in V\} &= \{\mathbf{c}'_2^{(T-1)}((k, j')) : k \in V\} \\ \{\mathbf{c}_2^{(T-1)}((i, k)) : k \in V\} &= \{\mathbf{c}'_2^{(T-1)}((i', k)) : k \in V\} \end{aligned} \tag{2}$$

The first condition, thanks to the inductive hypothesis, implies that $\tilde{h}_{i,j}^{(T-1)} = \tilde{h}_{i',j'}^{(T-1)}$. In particular, if $i \neq j$, then we have

$$\begin{aligned} a_{i,j} &= a'_{i',j'} \\ e_{i,j} &= e'_{i',j'} \end{aligned} \tag{3}$$

The third condition implies that \exists a permutation on V , which we can call $\xi_{i,i'}$, such that $\forall k \in V$,

$$\mathbf{c}_2^{(T-1)}((i, k)) = \mathbf{c}'_2^{(T-1)}((i', \xi_{i,i'}(k)))$$

By the inductive hypothesis, there is $\forall k \in V$,

$$\tilde{h}_{i,k}^{(T-1)} = \tilde{h}'_{i',\xi_{i,i'}(k)}^{(T-1)}$$

and moreover, $\xi_{i,i'}(k) = i'$ if and only if $k = i$. For $k \neq i$, we thus have

$$\begin{aligned} h_i^{(T-1)} &= h'_{i'}^{(T-1)} \\ h_k^{(T-1)} &= h'_{\xi_{i,i'}(k)}^{(T-1)} \\ a_{i,k} &= a'_{i',\xi_{i,i'}(k)} \\ e_{i,k} &= e'_{i',\xi_{i,i'}(k)} \end{aligned}$$

Now, looking at the update rule at the T th layer of the MPNN,

$$\begin{aligned} m_i^{(T)} &= \sum_{k \in \mathcal{N}(i)} M_T(h_i^{(T-1)}, h_k^{(T-1)}, e_{i,k}) \\ &= \sum_{k \in V} a_{i,k} \cdot M_T(h_i^{(T-1)}, h_k^{(T-1)}, e_{i,k}) \\ &= \sum_{k \in V} a'_{i',\xi_{i,i'}(k)} \cdot M_T(h'_{i'}^{(T-1)}, h'_{\xi_{i,i'}(k)}^{(T-1)}, e'_{i',\xi_{i,i'}(k)}) \\ &= \sum_{k' \in V} a'_{i',k'} \cdot M_T(h'_{i'}^{(T-1)}, h'_{k'}^{(T-1)}, e'_{i',k'}) \\ &= m'_{i'}^{(T)} \end{aligned}$$

where between the third and the fourth line we made the substitution $k' = \xi_{i,i'}(k)$. Therefore,

$$\begin{aligned} h_i^{(T)} &= U_t(h_i^{(T-1)}, m_i^{(T)}) \\ &= U_t(h'_{i'}^{(T-1)}, m'_{i'}^{(T)}) \\ &= h'_{i'}^{(T)} \end{aligned}$$

By the symmetry between i and j , we can also show that $h_j^{(T)} = h'_{j'}^{(T)}$. Hence, together with 3, we can conclude that

$$\tilde{h}_{i,j}^{(T)} = \tilde{h}'_{i',j'}^{(T)},$$

which proves the lemma. \square

Thus, the second result of this lemma tells us that $\forall i, j \in V^2$, $\tilde{h}_{i,j}^{(T_0)} = \tilde{h}'_{\eta_0(i,j)}^{(T_0)}$. Moreover, by the first result, \exists a permutation on V , which we can call τ_0 , such that $\forall i \in V$, $\eta((i, i)) = (\tau_0(i), \tau_0(i))$. Combining the two, we have that $\forall i \in V$, $h_i^{(T_0)} = h'_{\tau_0(i)}^{(T_0)}$, and hence

$$\{h_i^{(T_0)} : i \in V\} = \{h'_{i'}^{(T_0)} : i' \in V\} \quad (4)$$

Therefore, $\hat{y} = \hat{y}'$, meaning that the MPNN returns identical outputs on the two graphs. \square

D Proof of Theorem 2 (2-WL is unable to matching-count patterns of 3 or more nodes)

Proof. Say $G^{[P]} = (V^{[P]}, E^{[P]}, x^{[P]}, e^{[P]})$ is a connected pattern of m nodes, where $m > 2$, and thus $V^{[P]} = [m]$.

First, if $G^{[P]}$ is not a clique, then by definition, there exists two distinct nodes $i, j \in V^{[P]}$ such that i and j are not connected by an edge. Assume without loss of generality that $i = 1$ and $j = 2$. Now, construct two graphs $G^{[1]} = (V^{[1]}, E^{[1]}, x^{[1]}, e^{[1]})$, $G^{[2]} = (V^{[2]}, E^{[2]}, x^{[2]}, e^{[2]})$ both with $2m$ nodes. For $G^{[1]}$, let $E^{[1]} = \{(i, j) : i, j \leq m, (i, j) \in E^{[P]}\} \cup \{(i+m, j+m) : i, j \leq m, (i, j) \in E^{[P]}\} \cup \{(1, 2), (2, 1), (1+m, 2+m), (2+m, 1+m)\}$; $\forall i \leq m, x_i^{[1]} = x_{i+m}^{[1]} = x_i^{[P]}$; $\forall (i, j) \in E^{[P]}, e_{i,j}^{[1]} = e_{i+m,j+m}^{[1]} = e_{i,j}^{[P]}$, and moreover we can randomly choose a value of edge feature for $e_{1,2}^{[1]} = e_{2,1}^{[1]} = e_{1+m,2+m}^{[1]} = e_{2+m,1+m}^{[1]}$. For $G^{[2]}$, let $E^{[2]} = \{(i, j) : i, j \leq m, (i, j) \in E^{[P]}\} \cup \{(i+m, j+m) : i, j \leq m, (i, j) \in E^{[P]}\} \cup \{(1, 2+m), (2+m, 1), (1+m, 2), (2, 1+m)\}$; $\forall i \leq m, x_i^{[2]} = x_{i+m}^{[2]} = x_i^{[P]}$; $\forall (i, j) \in E^{[P]}, e_{i,j+m}^{[2]} = e_{i+m,j}^{[2]} = e_{i,j}^{[P]}$, and moreover we let $e_{1,2+m}^{[2]} = e_{2+m,1}^{[2]} = e_{1+m,2}^{[2]} = e_{2,1+m}^{[2]} = e_{1,2}^{[1]}$. In words, both $G^{[1]}$ and $G^{[2]}$ are constructed based on two copies of $G^{[P]}$, and the difference is that, $G^{[1]}$ adds the edges $\{(1, 2), (2, 1), (1+m, 2+m), (2+m, 1+m)\}$, whereas $G^{[2]}$ adds the edges $\{(1, 2+m), (2+m, 1), (1+m, 2), (2, 1+m)\}$, all with the same edge feature.

On one hand, by construction, 2-WL will not be able to distinguish $G^{[1]}$ from $G^{[2]}$. This is intuitive if we compare the rooted subtrees in the two graphs. Instead of giving a rigorous proof here, we note that this is a consequence of the direct proof of Corollary 4 given in Appendix I, in which we will show that the same pair of graphs cannot be distinguished by 2-IGNs. Since 2-IGNs are no less powerful than 2-WL (Maron et al., 2019b), this implies that 2-WL cannot distinguish them either.

On one hand, $G^{[1]}$ and $G^{[2]}$ has different matching-count of the pattern. $G^{[1]}$ contains no subgraph isomorphic to $G^{[P]}$. Intuitively this is obvious; to be rigorous, note that firstly, neither the subgraph induced by the nodes $\{1, \dots, m\}$ nor the subgraph induced by the nodes $\{1+m, \dots, 2m\}$ is isomorphic to $G^{[P]}$, and secondly, the subgraph induced by any other set of m nodes is not connected, whereas $G^{[P]}$ is connected. $G^{[2]}$, however, has at least two induced subgraphs isomorphic to $G^{[P]}$, one induced by the nodes $\{1, \dots, m\}$, and the other induced by the nodes $\{1+m, \dots, 2m\}$.

If $G^{[P]}$ is a clique, then we also first construct $G^{[1]}$, $G^{[2]}$ from $G^{[P]}$ as two copies of $G^{[P]}$. Then, for $G^{[1]}$, we pick two distinct nodes $1, 2 \in V^{[P]}$ and remove the edges $(1, 2), (2, 1), (1+m, 2+m)$ and $(2+m, 1+m)$ from $V^{[1]}$, while adding edges $(1, 2+m), (2+m, 1), (1+m, 2), (2, 1+m)$ with the same edge features. Then, $G^{[1]}$ contains no subgraph isomorphic to $G^{[P]}$, while $G^{[2]}$ contains two. Note that the pair of graphs is the same as the counterexample pair of graphs that could have been constructed in the non-clique case for the pattern that is a clique with one edge deleted. Hence 2-WL still cant distinguish $G^{[1]}$ from $G^{[2]}$. \square

E Proof of Theorem 3 (MPNNs are able to containment-count star-shaped patterns)

(See Section 2.1 of Arvind et al. (2018) for a proof for the case where all nodes have identical features.)

Proof. Without loss of generality, we represent a star-shaped pattern by $G^{[P]} = (V^{[P]}, E^{[P]}, x^{[P]}, e^{[P]})$, where $V^{[P]} = [m]$ (with node 1 representing the center) and $E^{[P]} = \{(1, i) : 2 \leq i \leq m\} \cup \{(i, 1) : 2 \leq i \leq m\}$. Given a graph G , for each of its node j , we define $N(j)$ as the set of its neighbors in the graph. Then the neighborhood centered at j contributes to $C_C(G, G^{[P]})$ if and only if $x_j = x_1^{[P]}$ and $\exists S \subseteq N(j)$ such that the multiset $\{(x_k, e_{jk}) : k \in S\}$ equals the multiset $\{(x_k^{[P]}, e_{1k}^{[P]}) : 2 \leq k \leq m\}$. Moreover, the contribution

to the number $C_C(G, G^{[P]})$ equals the number of all such subsets $S \subseteq N(j)$. Hence, we have the following decomposition

$$C_C(G, G^{[P]}) = \sum_{j \in V} f^{[P]} \left(x_j, \{(x_k, e_{jk}) : k \in N(j)\} \right),$$

where $f^{[P]}$, is defined for every 2-tuple consisting of a node feature and a multiset of pairs of node feature and edge feature (i.e., objects of the form

$$(x, M = \{(x_\alpha, e_\alpha) : \alpha \in K\})$$

where K is a finite set of indices) as

$$f^{[P]}(x, M) = \begin{cases} 0 & \text{if } x \neq x_1^{[P]} \\ \#_M^{[P]} & \text{if } x = x_1^{[P]} \end{cases}$$

where $\#_M^{[P]}$ denotes the number of sub-multisets of M that equals the multiset $\{(x_k^{[P]}, e_{1k}^{[P]}) : 2 \leq k \leq m\}$.

Thanks to Corollary 6 of [Xu et al. \(2018a\)](#) based on [Zaheer et al. \(2017\)](#), we know that $f^{[P]}$ can be expressed by some message-passing function in an MPNN. Thus, together with summation as the readout function, MPNN is able to express $C_C(G, G^{[P]})$. \square

F Proof of Theorem 4 (k -WL is able to count patterns of k or fewer nodes)

Proof. Suppose we run k -WL on two graphs, $G^{[1]}$ and $G^{[2]}$. In k -WL, the colorings of the k -tuples are initialized according to their isomorphism types as defined in Appendix B. Thus, if for some pattern of no more than k nodes, $G^{[1]}$ and $G^{[2]}$ have different matching-count or containment-count, then there exists an isomorphism type of k -tuples such that $G^{[1]}$ and $G^{[2]}$ differ in the number of k -tuples under this type. This implies that $\{c_k^{(0)}(s) : s \in (V^{[1]})^k\} \neq \{c_k^{(0)}(s') : s' \in (V^{[2]})^k\}$, and hence the two graphs can be distinguished at the 0th iteration of k -WL. \square

G Proof of Theorem 5 (T iterations of k -WL cannot matching-count path patterns of size $(k+1)2^T$ or more)

Proof. For any integer $m \geq (k+1)2^T$, we will construct two graphs $G^{[1]} = (V^{[1]} = [2m], E^{[1]}, x^{[1]}, e^{[1]})$ and $G^{[2]} = (V^{[2]} = [2m], E^{[2]}, x^{[2]}, e^{[2]})$, both with $2m$ nodes but with different matching-counts of H_m , and show that k -WL cannot distinguish them. Define $E_{double} = \{(i, i+1) : 1 \leq i < m\} \cup \{(i+1, i) : 1 \leq i < m\} \cup \{(i+m, i+m+1) : 1 \leq i < m\} \cup \{(i+m+1, i+m) : 1 \leq i < m\}$, which is the edge set of a graph that is exactly two disconnected copies of H_m . For $G^{[1]}$, let $E^{[1]} = E_{double} \cup \{(1, m), (m, 1), (1+m, 2m), (2m, 1+m)\}$; $\forall i \leq m, x_i^{[1]} = x_{i+m}^{[1]} = x_i^{[H_m]}$; $\forall (i, j) \in E^{[H_m]}, e_{i,j}^{[1]} = e_{j,i}^{[1]} = e_{i+m,j+m}^{[1]} = e_{j+m,i+m}^{[1]} = e_{i,j}^{[H_m]}$, and moreover, we can randomly choose a value of edge feature for $e_{1,m}^{[1]} = e_{m,1}^{[1]} = e_{1+m,2m}^{[1]} = e_{2m,1+m}^{[1]}$. For $G^{[2]}$, let $E^{[2]} = E_{double} \cup \{(1, 2m), (2m, 1), (m, 1+m), (1+m, 2m)\}$; $\forall i \leq m, x_i^{[2]} = x_{i+m}^{[2]} = x_i^{[H_m]}$; $\forall (i, j) \in E^{[H_m]}, e_{i,j}^{[2]} = e_{j,i}^{[2]} = e_{i+m,j+m}^{[2]} = e_{j+m,i+m}^{[2]} = e_{i,j}^{[H_m]}$, and moreover, set $e_{1,2m}^{[2]} = e_{2m,1}^{[2]} = e_{m,1+m}^{[2]} = e_{1+m,m}^{[2]} = e_{1,m}^{[1]}$. In words, both $G^{[1]}$ and $G^{[2]}$ are constructed based on two copies of H_m , and the difference is that, $G^{[1]}$ adds the edges $\{(1, m), (m, 1), (1+m, 2m), (2m, 1+m)\}$, whereas $G^{[2]}$ adds the edges $\{(1, 2m), (2m, 1), (m, 1+m), (1+m, m)\}$, all with the same edge feature. For the case $k=3, m=8, T=1$, for example, the constructed graphs are illustrated in Figure 4.

Can $G^{[1]}$ and $G^{[2]}$ be distinguished by k -WL? Let $\mathbf{c}_k^{(t)}, \mathbf{c}'_k^{(t)}$ be the coloring functions of k -tuples for $G^{[1]}$ and $G^{[2]}$, respectively, obtained after running k -WL on the two graphs simultaneously for t iterations. To show that the answer is negative, we want to show that

$$\{\mathbf{c}_k^{(T)}(s) : s \in [2m]^k\} = \{\mathbf{c}'_k^{(T)}(s) : s \in [2m]^k\} \quad (5)$$

To show this, it is sufficient to find a permutation $\eta : [2m]^k \rightarrow [2m]^k$ such that $\forall k\text{-tuple } s \in [2m]^k, \mathbf{c}_k^{(T)}(s) = \mathbf{c}'_k^{(T)}(\eta(s))$. Before defining such an η , we need the following lemma.

Lemma 4. *Let p be a positive integer. If $m \geq (k+1)p$, then $\forall s \in [2m]^k, \exists i \in [m]$ such that $\{i, i+1, \dots, i+p-1\} \cap \{\text{MOD}_m(j) : j \in s\} = \emptyset$.*

Proof of Lemma 4: We can use a simple counting argument to show this. For $u \in [k+1]$, define $A_u = \{up, up+1, \dots, (u+1)p-1\} \cup \{up+m, up+1+m, \dots, (u+1)p-1+m\}$. Then $|A_u| = 2p$, $A_u \cap A_{u'} = \emptyset$ if $u \neq u'$, and

$$[2m] \supseteq \bigcup_{u \in [k+1]} A_u, \quad (6)$$

since $m \geq (k+1)p$. Suppose that the claim is not true, then each A_i contains at least one node in s , and therefore

$$s \supseteq (s \cap [2m]) \supseteq \bigcup_{u \in [k+1]} (s \cap A_u),$$

which contains at least $k+1$ nodes, which is contradictory. \square

With this lemma, we see that $\forall s \in [2m]^k, \exists i \in [m]$ such that $\forall j \in s, \text{MOD}_m(j)$ either $< i$ or $\geq i + 2^{T+1} - 1$. Thus, we can first define the mapping $\chi : [2m]^k \rightarrow [m]$ from a k -tuple s to the smallest such node index $i \in [m]$. Next, $\forall i \in [m]$, we define a mapping τ_i from $[2m]$ to $[2m]$ as

$$\tau_i(j) = \begin{cases} j, & \text{if } \text{MOD}_m(j) \leq i \\ \text{MOD}_{2m}(j+m), & \text{otherwise} \end{cases} \quad (7)$$

τ_i is a permutation on $[2m]$. For $\forall i \in [m]$, this allows us to define a mapping ζ_i from $[2m]^k \rightarrow [2m]^k$ as, $\forall s = (i_1, \dots, i_k) \in [2m]^k$,

$$\zeta_i(s) = (\tau_i(i_1), \dots, \tau_i(i_k)). \quad (8)$$

Finally, we define a mapping η from $[2m]^k \rightarrow [2m]^k$ as,

$$\eta(s) = \zeta_{\chi(s)}(s) \quad (9)$$

The maps χ, τ and η are illustrated in Figure 4.

To fulfill the proof, there are two things we need to show about η . First, we want it to be a permutation on $[2m]^k$. To see this, observe that $\chi(s) = \chi(\eta(s))$, and hence $\forall s \in [2m]^k, (\eta \circ \eta)(s) = (\zeta_{\chi(\eta(s))} \circ \zeta_{\chi(s)})(s) = s$, since $\forall i \in [m], \tau_i \circ \tau_i$ is the identity map on $[2m]$.

Second, we need to show that $\forall s \in [2m]^k, \mathbf{c}_k^{(T)}(s) = \mathbf{c}'_k^{(T)}(\eta(s))$. This will be a consequence of the following lemma.

Lemma 5. *At iteration t , $\forall s \in [2m]^k, \forall i$ such that $\forall j \in s$, either $\text{MOD}_m(j) < i$ or $\text{MOD}_m(j) \geq i + 2^t$, there is*

$$\mathbf{c}_k^{(t)}(s) = \mathbf{c}'_k^{(t)}(\zeta_i(s)) \quad (10)$$

Remark: This statement allows i to depend on s , as will be the case when we apply this lemma to $\eta(s) = \zeta_{\chi(s)}(s)$, where we set i to be $\chi(s)$.

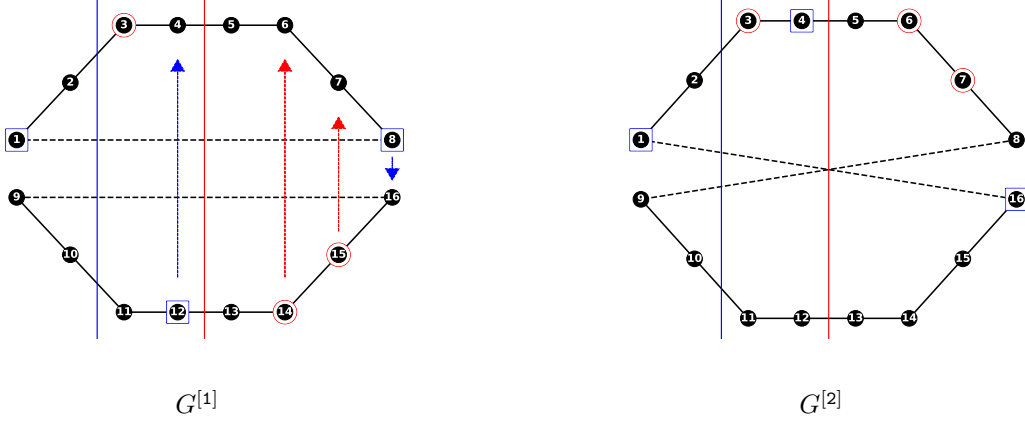


Figure 4: Illustration of the construction in the proof of Theorem 5 in Appendix G. In this particular case, $k = 3$, $m = 8$, $T = 1$. If we consider $s = (1, 12, 8)$ as an example, where the corresponding nodes are marked by blue squares in $G^{[1]}$, there is $\chi(s) = 2$, and thus $\eta(s) = \zeta_2(s) = (1, 4, 16)$, which are marked by blue squares in $G^{[2]}$. Similarly, if we consider $s = (3, 14, 15)$, then $\chi(s) = 4$, and thus $\eta(s) = \zeta_4(s) = (3, 6, 7)$. In both cases, we see that the isomorphism type of s in $G^{[1]}$ equals the isomorphism type of $\eta(s)$ in $G^{[2]}$. In the end, we will show that $\mathbf{c}_k^{(T)}(s) = \mathbf{c}_k^{(T)}(\eta(s))$.

Proof of Lemma 5: Notation-wise, for any k -tuple, $s = (i_1, \dots, i_k)$, and for $w \in [k]$, use $\mathbf{I}_w(s)$ to denote the w th entry of s , i_w .

The lemma can be shown by using induction on t . Before looking at the base case $t = 0$, we will first show the inductive step, which is:

$$\begin{aligned} \forall \bar{T}, \text{ suppose the lemma holds for all } t \leq \bar{T} - 1, \\ \text{then it also holds for } t = \bar{T}. \end{aligned} \quad (11)$$

Inductive step:

Fix a \bar{T} and suppose the lemma holds for all $t \leq \bar{T} - 1$. Under the condition that $\forall j \in s$, either $\text{MOD}_m(j) < i$ or $\text{MOD}_m(j) \geq i + 2^{\bar{T}}$, to show $\mathbf{c}_k^{(\bar{T})}(s) = \mathbf{c}_k^{(\bar{T})}(\zeta_i(s))$, we need two things to hold:

1. $\mathbf{c}_k^{(\bar{T}-1)}(s) = \mathbf{c}_k^{(\bar{T}-1)}(\zeta_i(s))$
2. $\forall w \in [k], \{\mathbf{c}_k^{(\bar{T}-1)}(\tilde{s}) : \tilde{s} \in N_w(s)\} = \{\mathbf{c}_k^{(\bar{T}-1)}(\tilde{s}) : \tilde{s} \in N_w(\zeta_i(s))\}$

The first condition is a consequence of the inductive hypothesis, as $i + 2^{\bar{T}} > i + 2^{(\bar{T}-1)}$. For the second condition, it is sufficient to find for all $w \in [k]$, a bijective mapping ξ from $N_w(s)$ to $N_w(\zeta_i(s))$ such that $\forall \tilde{s} \in N_w(s)$, $\mathbf{c}_k^{(\bar{T}-1)}(\tilde{s}) = \mathbf{c}_k^{(\bar{T}-1)}(\xi(\tilde{s}))$.

We then define $\beta(i, \tilde{s}) =$

$$\begin{cases} \text{MOD}_m(\mathbf{I}_w(\tilde{s})) + 1, & \text{if } i \leq \text{MOD}_m(\mathbf{I}_w(\tilde{s})) < i + 2^{\bar{T}-1} \\ i, & \text{otherwise} \end{cases} \quad (12)$$

Now, consider any $\tilde{s} \in N_w(s)$. Note that \tilde{s} and s differ only in the w th entry of the k -tuple.

- If $i \leq \text{MOD}_m(\mathbf{I}_w(\tilde{s})) < i + 2^{\bar{T}-1}$, then $\forall j \in \tilde{s}$,

- either $j \in s$, in which case either $\text{MOD}_m(j) < i < \text{MOD}_m(\mathbf{I}_w(\tilde{s})) + 1 = \beta(i, \tilde{s})$ or $\text{MOD}_m(j) \geq i + 2^{\bar{T}} \geq \text{MOD}_m(\mathbf{I}_w(\tilde{s})) + 1 + 2^{\bar{T}-1} = \beta(i, \tilde{s}) + 2^{\bar{T}-1}$,
- or $j = \mathbf{I}_w(\tilde{s})$, in which case $\text{MOD}_m(j) < \text{MOD}_m(\mathbf{I}_w(\tilde{s})) + 1 = \beta(i, \tilde{s})$.
- If $\text{MOD}_m(\mathbf{I}_w(\tilde{s})) < i$ or $\text{MOD}_m(\mathbf{I}_w(\tilde{s})) \geq i + 2^{\bar{T}-1}$, then $\forall j \in \tilde{s}$,
 - either $j \in s$, in which case either $\text{MOD}_m(j) < i = \beta(i, \tilde{s})$ or $\text{MOD}_m(j) \geq i + 2^{\bar{T}} \geq \beta(i, \tilde{s}) + 2^{\bar{T}-1}$,
 - or $j = \mathbf{I}_w(\tilde{s})$, in which case either $\text{MOD}_m(j) < i = \beta(i, \tilde{s})$ or $\text{MOD}_m(j) \geq i + 2^{\bar{T}-1} \geq \beta(i, \tilde{s}) + 2^{\bar{T}-1}$.

Thus, in all cases, there is $\forall j \in \tilde{s}$, either $\text{MOD}_m(j) < \beta(i, \tilde{s})$, or $\text{MOD}_m(j) \geq i + 2^{\bar{T}-1}$. Hence, by the inductive hypothesis, we have $\mathbf{c}_k^{(\bar{T}-1)}(\tilde{s}) = \mathbf{c}_k'^{(\bar{T}-1)}(\zeta_{\beta(i, \tilde{s})}(\tilde{s}))$. This inspires us to define, for $\forall w \in [k]$, $\forall \tilde{s} \in N_w(s)$,

$$\xi(\tilde{s}) = \zeta_{\beta(i, \tilde{s})}(\tilde{s}) \quad (13)$$

Additionally, we still need to prove that, firstly, ξ maps $N_w(s)$ to $N_w(\zeta_i(s))$, and secondly, ξ is a bijection. For the first statement, note that $\forall \tilde{s} \in N_w(s)$, $\zeta_{\beta(i, \tilde{s})}(s) = \zeta_i(s)$ because s contains no entry between i and $\beta(i, \tilde{s})$, with the latter being less than $i + 2^{\bar{T}}$. Hence, if $\tilde{s} \in N_w(s)$, then $\forall w' \in [k]$ with $w' \neq w$, there is $\mathbf{I}_{w'}(\tilde{s}) = \mathbf{I}_{w'}(s)$, and therefore $\mathbf{I}_{w'}(\xi(\tilde{s})) = \mathbf{I}_{w'}(\zeta_{\beta(i, \tilde{s})}(\tilde{s})) = \tau_{\beta(i, \tilde{s})}(\mathbf{I}_{w'}(\tilde{s})) = \tau_{\beta(i, \tilde{s})}(\mathbf{I}_{w'}(s)) = \mathbf{I}_{w'}(\zeta_{\beta(i, \tilde{s})}(s)) = \mathbf{I}_{w'}(\zeta_i(s))$, which ultimately implies that $\xi(\tilde{s}) \in N_w(\zeta_i(s))$.

For the second statement, note that since $\mathbf{I}_w(\xi(\tilde{s})) = \tau_{\beta(i, \tilde{s})}(\mathbf{I}_w(\tilde{s}))$ (by the definition of ζ), there is $\text{MOD}_m(\mathbf{I}_w(\xi(\tilde{s}))) = \text{MOD}_m(\tau_{\beta(i, \tilde{s})}(\mathbf{I}_w(\tilde{s}))) = \text{MOD}_m(\mathbf{I}_w(\tilde{s}))$, and therefore $\beta(i, \xi(\tilde{s})) = \beta(i, \tilde{s})$. Thus, we know that $(\xi \circ \xi)(\tilde{s}) = (\zeta_{\beta(i, \xi(\tilde{s}))} \circ \zeta_{\beta(i, \tilde{s})})(\tilde{s}) = (\zeta_{\beta(i, \tilde{s})} \circ \zeta_{\beta(i, \tilde{s})})(\tilde{s}) = \tilde{s}$. This implies that ξ is a bijection from $N_w(s)$ to $N_w(\zeta_i(s))$.

This concludes the proof of the inductive step.

Base case:

We need to show that

$$\begin{aligned} \forall s \in [2m]^k, \forall i^* \text{ such that } \forall j \in s, \text{ either } \text{MOD}_m(j) < i^* \\ \text{or } \text{MOD}_m(j) \geq i^* + 1, \text{ there is } \mathbf{c}_k^{(0)}(s) = \mathbf{c}_k'^{(0)}(\zeta_{i^*}(s)) \end{aligned} \quad (14)$$

By the way in which the colorings of the k -tuples are initialized in k -WL, the statement above is equivalent to showing that s in $G^{[1]}$ and $\zeta_{i^*}(s)$ in $G^{[2]}$ have the same isomorphism type, for which we need the following to hold.

Lemma 6. *Say $s = (i_1, \dots, i_k)$, in which case $\zeta_{i^*}(s) = (\tau_{i^*}(i_1), \dots, \tau_{i^*}(i_k))$. Then*

1. $\forall i_\alpha, i_\beta \in s, i_\alpha = i_\beta \Leftrightarrow \tau_{i^*}(i_\alpha) = \tau_{i^*}(i_\beta)$
2. $\forall i_\alpha \in s, x_{i_\alpha}^{[1]} = x_{\tau_{i^*}(i_\alpha)}^{[2]}$
3. $\forall i_\alpha, i_\beta \in s, (i_\alpha, i_\beta) \in E^{[1]} \Leftrightarrow (\tau_{i^*}(i_\alpha), \tau_{i^*}(i_\beta)) \in E^{[2]}$, and moreover, if either is true, $e_{i_\alpha, i_\beta}^{[1]} = e_{\tau_{i^*}(i_\alpha), \tau_{i^*}(i_\beta)}^{[2]}$

Proof of Lemma 6:

1. This is true since τ_{i^*} is a permutation on $[2m]$.
2. This is true because by the construction of the two graphs, $\forall i \in [2m], x_i^{[1]} = x_i^{[2]}$, and moreover $x_i^{[1]} = x_{i+m}^{[1]}$ if $i \leq m$.

3. Define $S = \{(1, m), (m, 1), (1 + m, 2m), (2m, 1 + m), (1, 2m), (2m, 1), (m, 1 + m), (1 + m, 2m)\}$, which is the set of “special” pairs of nodes in which $G^{[1]}$ and $G^{[2]}$ differ. Note that $\forall (i_\alpha, i_\beta) \in [2m]^2, (i_\alpha, i_\beta) \in S$ if and only if the sets $\{\text{MOD}_m(i_\alpha), \text{MOD}_m(i_\beta)\} = \{1, m\}$.

By the assumption on i^* in (14), we know that $i_\alpha, i_\beta \notin \{i^*, i^* + m\}$. Now we look at 16 different cases separately, which comes from 4 possibilities for each of i_α and i_β : i_α (or i_β) belonging to $\{1, \dots, i^* - 1\}, \{i^* + 1, \dots, m\}, \{1 + m, \dots, i^* - 1 + m\}$, or $\{i^* + 1 + m, \dots, 2m\}$

Case 1 $1 \leq i_\alpha, i_\beta < i^*$

Then $\tau_{i^*}(i_\alpha) = i_\alpha, \tau_{i^*}(i_\beta) = i_\beta$. In addition, as $\text{MOD}_m(i_\alpha), \text{MOD}_m(i_\beta) \neq m$, there is $(i_\alpha, i_\beta) \notin S$. Thus, if $(i_\alpha, i_\beta) \in E^{[1]}$, then $(i_\alpha, i_\beta) \in E_{\text{double}} \subset E^{[2]}$, and moreover, $e_{i_\alpha, i_\beta}^{[1]} = e_{i_\alpha, i_\beta}^{[\mathbb{H}_m]} = e_{i_\alpha, i_\beta}^{[2]} = e_{\tau_{i^*}(i_\alpha), \tau_{i^*}(i_\beta)}^{[2]}$. Same for the other direction.

Case 2 $1 + m \leq i_\alpha, i_\beta < i^* + m$

Similar to case 1.

Case 3 $i^* + 1 \leq i_\alpha, i_\beta \leq m$

Then $\tau_{i^*}(i_\alpha) = i_\alpha + m, \tau_{i^*}(i_\beta) = i_\beta + m$. In addition, as $\text{MOD}_m(i_\alpha), \text{MOD}_m(i_\beta) \neq 1$, there is $(i_\alpha, i_\beta) \notin S$. Thus, if $(i_\alpha, i_\beta) \in E^{[1]}$, then $(i_\alpha, i_\beta) \in E_{\text{double}}$, and hence $(i_\alpha + m, i_\beta + m) \in E_{\text{double}} \subset E^{[2]}$, and moreover, $e_{i_\alpha, i_\beta}^{[1]} = e_{i_\alpha, i_\beta}^{[\mathbb{H}_m]} = e_{i_\alpha + m, i_\beta + m}^{[2]} = e_{\tau_{i^*}(i_\alpha), \tau_{i^*}(i_\beta)}^{[2]}$.

Case 4 $i^* + 1 + m \leq i_\alpha, i_\beta \leq 2m$

Similar to case 3.

Case 5 $1 \leq i_\alpha < i^*, i^* + 1 \leq i_\beta \leq m$

If $i_\alpha \neq 1$ or $i_\beta \neq m$, then since H_m is a path and $i_\alpha < i^* \leq i_\beta - 1$, $(i_\alpha, i_\beta) \notin E^{[1]}$ or $E^{[2]}$. Now we consider the case where $i_\alpha = 1, i_\beta = m$. As $1 \leq i^* < m$, by the definition of τ , there is $\tau_{i^*}(1) = 1$, and $\tau_{i^*}(m) = 2m$. Note that both $(1, m) \in E^{[1]}$ and $(1, 2m) \in E^{[2]}$ are true, and moreover, $e_{1, m}^{[1]} = e_{1, 2m}^{[2]}$.

Case 6 $1 \leq i_\beta < i^*, i^* + 1 \leq i_\alpha \leq m$

Similar to case 5.

Case 7 $1 + m \leq i_\alpha < i^* + m, i^* + 1 + m \leq i_\beta \leq 2m$

Similar to case 5.

Case 8 $1 + m \leq i_\beta < i^* + m, i^* + 1 + m \leq i_\alpha \leq 2m$

Similar to case 5.

Case 9 $1 \leq i_\alpha < i^*$ and $1 + m \leq i_\beta < i^* + m$

Then $\tau_s(i_\alpha) = i_\alpha, \tau_s(i_\beta) = i_\beta$, and $(i_\alpha, i_\beta) \notin E^{[1]}$ or $E^{[2]}$.

Case 10 $1 \leq i_\beta < i^*$ and $1 + m \leq i_\alpha < i^* + m$

Similar to case 9.

Case 11 $i^* + 1 \leq i_\alpha < m$ and $i^* + 1 + m \leq i_\beta \leq 2m$

$(i_\alpha, i_\beta) \notin E^{[1]}$. $\tau_s(i_\alpha) = i_\alpha + m, \tau_s(i_\beta) = i_\beta - m$. Hence $(\tau_s(i_\alpha), \tau_s(i_\beta)) \notin E^{[2]}$ either.

Case 12 $i^* + 1 \leq i_\beta \leq m$ and $i^* + 1 + m \leq i_\alpha \leq 2m$

Similar to case 11.

Case 13 $1 \leq i_\alpha < i^*$ and $i^* + 1 + m \leq i_\beta \leq 2m$

$(i_\alpha, i_\beta) \notin E^{[1]}$ obviously. We also have $\tau_s(i_\alpha) = i_\alpha \in [1, i^*]$, $\tau_s(i_\beta) = i_\beta - 1 \in [i^* + 1, m]$, and hence $(\tau_s(i_\alpha), \tau_s(i_\beta)) \notin E^{[2]}$.

Case 14 $1 \leq i_\beta < i^*$ and $i^* + 1 + m \leq i_\alpha \leq 2m$

Similar to case 13.

Case 15 $1 + m \leq i_\alpha < i^* + m$ and $i^* + 1 \leq i_\beta \leq m$

Similar to case 13.

Case 16 $1 + m \leq i_\beta < i^* + m$ and $i^* + 1 \leq i_\alpha \leq m$
 Similar to case 13.

This concludes the proof of Lemma 6. \square

Lemma 6 completes the proof of the base case, and hence the induction argument for Lemma 5. \square

$\forall s \in [2m]^k$, since $\eta(s) = \zeta_{\chi(s)}(s)$, and $\chi(s)$ satisfies $\forall j \in s$, either $\text{MOD}_m(j) < i$ or $\text{MOD}_m(j) \geq i + 2^T$, Lemma 5 implies that at iteration T , we have $\mathbf{c}_k^{(T)}(s) = \mathbf{c}'_k^{(T)}(\zeta_{\chi(s)}(s)) = \mathbf{c}'_k^{(T)}(\eta(s))$. Since we have shown that η is a permutation on $[2m]^k$, this let's us conclude that

$$\{\mathbf{c}_k^{(T)}(s) : s \in [2m]^k\} = \{\mathbf{c}'_k^{(T)}(s) : s \in [2m]^k\}, \quad (15)$$

and therefore k -WL cannot distinguish between the two graphs in T iterations. \square

H Proof of Theorem 6 (2-IGNs are no more powerful than 2-WL)

Proof. For simplicity of notations, we assume $d_t = 1$ in every layer of a 2-IGN. The general case can be proved by adding more subscripts. For 2-WL, we use the definition in section 3.1 except for omitting the subscript k in $\mathbf{c}_k^{(t)}$.

To start, it is straightforward to show (and we will prove it at the end) that the theorem can be deduced from the following lemma:

Lemma 7. *Say $G^{[1]}$ and $G^{[2]}$ cannot be distinguished by the 2-WL. Then $\forall t \in \mathbb{N}$, it holds that*

$$\forall s, s' \in V^2, \text{ if } \mathbf{c}^{(t)}(s) = \mathbf{c}'^{(t)}(s'), \text{ then } \mathbf{B}_s^{(t)} = \mathbf{B}'_{s'}^{(t)} \quad (16)$$

This lemma can be shown by induction. To see this, first note that the lemma is equivalent to the statement that

$$\forall T \in \mathbb{N}, \forall t \leq T, (16) \text{ holds.}$$

This allows us to carry out an induction in $T \in \mathbb{N}$. For the base case $t = T = 0$, this is true because $\mathbf{c}^{(0)}$ and $\mathbf{c}'^{(0)}$ in WL and $\mathbf{B}^{(0)}$ and $\mathbf{B}'^{(0)}$ in 2-IGN are both initialized in the same way according to the subgraph isomorphism. To be precise, $\mathbf{c}^{(0)}(s) = \mathbf{c}'^{(0)}(s')$ if and only if the subgraph in $G^{[1]}$ induced by the pair of nodes s is isomorphic to the subgraph in $G^{[2]}$ induced by the pair of nodes s' , which is also true if and only if $\mathbf{B}_s^{(0)} = \mathbf{B}'_{s'}^{(0)}$.

Next, to show that the induction step holds, we need to prove the following statement:

$$\begin{aligned} \forall T \in \mathbb{N}, \text{ if } \forall t \leq T-1, (16) \text{ holds,} \\ \text{then } (16) \text{ also holds for } t = T. \end{aligned}$$

To prove the consequent, we assume that for some $s, s' \in V^2$, there is $\mathbf{c}^{(T)}(s) = \mathbf{c}'^{(T)}(s')$, and then attempt to show that $\mathbf{B}_s^{(T)} = \mathbf{B}'_{s'}^{(T)}$. By the update rules of k -WL, the statement $\mathbf{c}^{(T)}(s) = \mathbf{c}'^{(T)}(s')$ implies that

$$\begin{cases} \mathbf{c}^{(T-1)}(s) = \mathbf{c}'^{(T-1)}(s') \\ \{\mathbf{c}^{(T-1)}(\tilde{s}) : \tilde{s} \in N_1(s)\} = \{\mathbf{c}'^{(T-1)}(\tilde{s}) : \tilde{s} \in N_1(s')\} \\ \{\mathbf{c}^{(T-1)}(\tilde{s}) : \tilde{s} \in N_2(s)\} = \{\mathbf{c}'^{(T-1)}(\tilde{s}) : \tilde{s} \in N_2(s')\} \end{cases} \quad (17)$$

Case 1: $s = (i, j) \in V^2$ **with** $i \neq j$

Let's first consider the case where $s = (i, j) \in V^2$ with $i \neq j$. In this case, we can also write $s' = (i', j') \in V^2$ with $i' \neq j'$, thanks to Lemma 2. Then, note that V^2 can be written as the union of 9 disjoint sets that are defined depending on s :

$$V^2 = \bigcup_{w=1}^9 A_{s,w},$$

where we define $A_{s,1} = \{(i, j)\}$, $A_{s,2} = \{(i, i)\}$, $A_{s,3} = \{(j, j)\}$, $A_{s,4} = \{(i, k) : k \neq i \text{ or } j\}$, $A_{s,5} = \{(k, i) : k \neq i \text{ or } j\}$, $A_{s,6} = \{(j, k) : k \neq i \text{ or } j\}$, $A_{s,7} = \{(k, j) : k \neq i \text{ or } j\}$, $A_{s,8} = \{(k, l) : k \neq l \text{ and } \{k, l\} \cap \{i, j\} = \emptyset\}$, and $A_{s,9} = \{(k, k) : k \notin \{i, j\}\}$. In this way, we partition V^2 into 9 different subsets, each of which consisting of pairs (k, l) that yield a particular equivalence class of the 4-tuple (i, j, k, l) . Similarly, we can define $A_{s',w}$ for $w \in [9]$, which will also give us

$$V^2 = \bigcup_{w=1}^9 A_{s',w}$$

Moreover, note that

$$N_1(s) = \bigcup_{w=1,3,7} A_{s,w}$$

$$N_2(s) = \bigcup_{w=1,2,4} A_{s,w}$$

$$N_1(s') = \bigcup_{w=1,3,7} A_{s',w}$$

$$N_2(s') = \bigcup_{w=1,2,4} A_{s',w}$$

Before proceeding, we make the following definition to simplify notations:

$$\mathfrak{C}_{s,w} = \{c^{(T-1)}(\tilde{s}) : \tilde{s} \in A_{s,w}\}$$

$$\mathfrak{C}'_{s',w} = \{c'^{(T-1)}(\tilde{s}) : \tilde{s} \in A_{s',w}\}$$

This allows us to rewrite (17) as

$$\mathfrak{C}_{s,1} = \mathfrak{C}'_{s',1} \tag{18}$$

$$\bigcup_{w=1,3,7} \mathfrak{C}_{s,w} = \bigcup_{w=1,3,7} \mathfrak{C}'_{s',w} \tag{19}$$

$$\bigcup_{w=1,2,4} \mathfrak{C}_{s,w} = \bigcup_{w=1,2,4} \mathfrak{C}'_{s',w} \tag{20}$$

Combining (18) and (19), we obtain

$$\bigcup_{w=3,7} \mathfrak{C}_{s,w} = \bigcup_{w=3,7} \mathfrak{C}'_{s',w} \tag{21}$$

Combining (18) and (20), we obtain

$$\bigcup_{w=2,4} \mathfrak{C}_{s,w} = \bigcup_{w=2,4} \mathfrak{C}'_{s',w} \tag{22}$$

Note that V^2 can also be partitioned into two disjoint subsets:

$$V^2 = \left(\bigcup_{w=1,4,5,6,7,8} A_{s,w} \right) \cap \left(\bigcup_{w=2,3,9} A_{s,w} \right),$$

where the first subset represent the edges: $\{(i, j) \in V^2 : i \neq j\}$ and the second subset represent the nodes: $\{(i, i) : i \in V\}$. Similarly,

$$V^2 = \left(\bigcup_{w=1,4,5,6,7,8} A_{s',w} \right) \cap \left(\bigcup_{w=2,3,9} A_{s',w} \right),$$

As shown in Lemma 2, pairs of nodes that represent edges cannot share the same color with pairs of nodes the represent nodes in any iteration of 2-WL. Thus, we have

$$\left(\bigcup_{w=1,4,5,6,7,8} \mathfrak{C}_{s,w} \right) \cap \left(\bigcup_{w=2,3,9} \mathfrak{C}'_{s',w} \right) = \emptyset \quad (23)$$

$$\left(\bigcup_{w=1,4,5,6,7,8} \mathfrak{C}'_{s',w} \right) \cap \left(\bigcup_{w=2,3,9} \mathfrak{C}_{s,w} \right) = \emptyset \quad (24)$$

Combining (21) and (23) or (24), we get

$$\mathfrak{C}_{s,3} = \mathfrak{C}'_{s',3} \quad (25)$$

$$\mathfrak{C}_{s,7} = \mathfrak{C}'_{s',7} \quad (26)$$

Combining (22) and (23) or (24), we get

$$\mathfrak{C}_{s,2} = \mathfrak{C}'_{s',2} \quad (27)$$

$$\mathfrak{C}_{s,4} = \mathfrak{C}'_{s',4} \quad (28)$$

Thanks to symmetry between (i, j) and (j, i) , as we work with undirected graphs, there is

$$\mathfrak{C}_{s,5} = \mathfrak{C}_{s,4} = \mathfrak{C}'_{s',4} = \mathfrak{C}'_{s',5} \quad (29)$$

$$\mathfrak{C}_{s,6} = \mathfrak{C}_{s,7} = \mathfrak{C}'_{s',7} = \mathfrak{C}'_{s',6} \quad (30)$$

In addition, since we assume that $G^{[1]}$ and $G^{[2]}$ cannot be distinguished by 2-WL, there has to be

$$\bigcup_{w=1}^9 \mathfrak{C}_{s,w} = \bigcup_{w=1}^9 \mathfrak{C}'_{s',w} \quad (31)$$

Combining this with (23) or (24), we get

$$\bigcup_{w=1,4,5,6,7,8} \mathfrak{C}_{s,w} = \bigcup_{w=1,4,5,6,7,8} \mathfrak{C}'_{s',w} \quad (32)$$

$$\bigcup_{w=2,3,9} \mathfrak{C}_{s,w} = \bigcup_{w=2,3,9} \mathfrak{C}'_{s',w} \quad (33)$$

Combining (32) with (18), (28), (29), (30), (26), we get

$$\mathfrak{C}_{s,8} = \mathfrak{C}'_{s',8} \quad (34)$$

Combining (33) with (27) and (25), we get

$$\mathfrak{C}_{s,9} = \mathfrak{C}'_{s',9} \quad (35)$$

Hence, in conclusion, we have that $\forall w \in [9]$,

$$\mathfrak{C}_{s,w} = \mathfrak{C}'_{s',w} \quad (36)$$

By the inductive hypothesis, this implies that $\forall w \in [9]$,

$$\{\mathbf{B}_{\tilde{s}}^{(T-1)} : \tilde{s} \in A_{s,w}\} = \{\mathbf{B}'_{\tilde{s}}^{(T-1)} : \tilde{s} \in A_{s',w}\} \quad (37)$$

Let us show how (37) may be leveraged. First, to prove that $\mathbf{B}_s^{(T)} = \mathbf{B}_{s'}^{(T)}$, recall that

$$\begin{aligned}\mathbf{B}^{(T)} &= \sigma(L^{(T)}(\mathbf{B}^{(T-1)})) \\ \mathbf{B}'^{(T)} &= \sigma(L^{(T)}(\mathbf{B}'^{(T-1)}))\end{aligned}\tag{38}$$

Therefore, it is sufficient to show that for all linear equivariant layer L , we have

$$L(\mathbf{B}^{(T-1)})_{i,j} = L(\mathbf{B}'^{(T-1)})_{i',j'}\tag{39}$$

Also, recall that

$$\begin{aligned}L(\mathbf{B}^{(T-1)})_{i,j} &= \sum_{(k,l) \in V^2} T_{i,j,k,l} \mathbf{B}_{k,l} + Y_{i,j} \\ L(\mathbf{B}'^{(T-1)})_{i',j'} &= \sum_{(k',l') \in V^2} T_{i',j',k',l'} \mathbf{B}'_{k',l'} + Y_{i',j'}\end{aligned}\tag{40}$$

By the definition of the $A_{s,w}$'s and $A_{s',w}$'s, there is $\forall w \in [9], \forall (k,l) \in A_{s,w}, \forall (k',l') \in A_{s',w}$, we have the 4-tuples $(i,j,k,l) \sim (i',j',k',l')$, i.e., \exists a permutation π on V such that $(i,j,k,l) = (\pi(i'), \pi(j'), \pi(k'), \pi(l'))$, which implies that $T_{i,j,k,l} = T_{i',j',k',l'}$. Therefore, together with (37), we have the following:

$$\begin{aligned}L(\mathbf{B}^{(T-1)})_{i,j} &= \sum_{(k,l) \in V^2} T_{i,j,k,l} \mathbf{B}_{k,l} + Y_{i,j} \\ &= \sum_{w=1}^9 \sum_{(k,l) \in A_{s,w}} T_{i,j,k,l} \mathbf{B}_{k,l} + Y_{i,j} \\ &= \sum_{w=1}^9 \sum_{(k',l') \in A_{s',w}} T_{i',j',k',l'} \mathbf{B}'_{k',l'} + Y_{i',j'} \\ &= L(\mathbf{B}'^{(T-1)})_{i',j'}\end{aligned}\tag{41}$$

and hence $\mathbf{B}_{i,j}^{(T)} = \mathbf{B}_{i',j'}^{(T)}$, which concludes the proof for the case that $s = (i,j)$ for $i \neq j$.

Case 2: $s = (i,i) \in V^2$

Next, consider the case $s = (i,i) \in V^2$. In this case, $s' = (i',i')$ for some $i' \in V$. This time, we write V^2 as the union of 5 disjoint sets that depend on s (or s'):

$$V^2 = \bigcup_{w=1}^5 A_{s,w},$$

where we define $A_{s,1} = \{(i,i)\}$, $A_{s,2} = \{(i,j) : j \neq i\}$, $A_{s,3} = \{(j,i) : j \neq i\}$, $A_{s,4} = \{(j,k) : j, k \neq i \text{ and } j \neq k\}$, and $A_{s,5} = \{(j,j) : j \neq i\}$. Similar for s' . We can also define $\mathfrak{C}_{s,w}$ and $\mathfrak{C}'_{s',w}$ as above. Note that

$$\begin{aligned}N_1(s) &= \bigcup_{w=1,3} A_{s,w} \\ N_2(s) &= \bigcup_{w=1,2} A_{s,w} \\ N_1(s') &= \bigcup_{w=1,3} A_{s',w} \\ N_2(s') &= \bigcup_{w=1,2} A_{s',w}\end{aligned}$$

Hence, we can rewrite (17) as

$$\mathfrak{C}_{s,1} = \mathfrak{C}'_{s',1} \quad (42)$$

$$\bigcup_{w=1,3} \mathfrak{C}_{s,w} = \bigcup_{w=1,3} \mathfrak{C}'_{s',w} \quad (43)$$

$$\bigcup_{w=1,2} \mathfrak{C}_{s,w} = \bigcup_{w=1,2} \mathfrak{C}'_{s',w} \quad (44)$$

Combining (42) with (43), we get

$$\mathfrak{C}_{s,3} = \mathfrak{C}'_{s',3} \quad (45)$$

Combining (42) with (44), we get

$$\mathfrak{C}_{s,2} = \mathfrak{C}'_{s',2} \quad (46)$$

Moreover, since we can decompose V^2 as

$$\begin{aligned} V^2 &= \left(\bigcup_{w=1,5} A_{s,w} \right) \cup \left(\bigcup_{w=2,3,4} A_{s,w} \right) \\ &= \left(\bigcup_{w=1,5} A_{s',w} \right) \cup \left(\bigcup_{w=2,3,4} A_{s',w} \right) \end{aligned}$$

with $\bigcup_{w=1,5} A_{s,w} = \bigcup_{w=1,5} A_{s',w}$ representing the nodes and $\bigcup_{w=2,3,4} A_{s,w} = \bigcup_{w=2,3,4} A_{s',w}$ representing the edges, we have

$$\left(\bigcup_{w=1,5} \mathfrak{C}_{s,w} \right) \cap \left(\bigcup_{w=2,3,4} \mathfrak{C}'_{s',w} \right) = \emptyset \quad (47)$$

$$\left(\bigcup_{w=1,5} \mathfrak{C}'_{s',w} \right) \cap \left(\bigcup_{w=2,3,4} \mathfrak{C}_{s,w} \right) = \emptyset \quad (48)$$

Since $G^{[1]}$ and $G^{[2]}$ cannot be distinguished by 2-WL, there is

$$\bigcup_{w=1}^5 \mathfrak{C}_{s,w} = \bigcup_{w=1}^5 \mathfrak{C}'_{s',w} \quad (49)$$

Therefore, combining with (47) or (48), we obtain

$$\bigcup_{w=1,5} \mathfrak{C}_{s,w} = \bigcup_{w=1,5} \mathfrak{C}'_{s',w} \quad (50)$$

$$\bigcup_{w=2,3,4} \mathfrak{C}_{s,w} = \bigcup_{w=2,3,4} \mathfrak{C}'_{s',w} \quad (51)$$

Combining (50) with (42), we get

$$\mathfrak{C}_{s,5} = \mathfrak{C}'_{s',5} \quad (52)$$

Combining (51) with (46) and (45), we get

$$\mathfrak{C}_{s,4} = \mathfrak{C}'_{s',4} \quad (53)$$

Hence, in conclusion, we have that $\forall w \in [5]$,

$$\mathfrak{C}_{s,w} = \mathfrak{C}'_{s',w} \quad (54)$$

By the inductive hypothesis, this implies that $\forall w \in [5]$,

$$\{\mathbf{B}_{\tilde{s}}^{(T-1)} : \tilde{s} \in A_{s,w}\} = \{\mathbf{B}'_{\tilde{s}}^{(T-1)} : \tilde{s} \in A_{s',w}\} \quad (55)$$

Thus,

$$\begin{aligned}
L(\mathbf{B}^{(T-1)})_{i,i} &= \sum_{(k,l) \in V^2} T_{i,i,k,l} \mathbf{B}_{k,l} + Y_{i,i} \\
&= \sum_{w=1}^5 \sum_{(k,l) \in A_{s,w}} T_{i,i,k,l} \mathbf{B}_{k,l} + Y_{i,i} \\
&= \sum_{w=1}^5 \sum_{(k',l') \in A_{s',w}} T_{i',i',k',l'} \mathbf{B}'_{k',l'} + Y_{i',i'} \\
&= L(\mathbf{B}'^{(T-1)})_{i',i'}
\end{aligned}$$

and hence $\mathbf{B}_{i,j}^{(T)} = \mathbf{B}'_{i',j'}^{(T)}$, which concludes the proof for the case that $s = (i, i)$ for $i \in V$. \square

Now, suppose we are given any 2-IGN with T layers. Since $G^{[1]}$ and $G^{[2]}$ cannot be distinguished by 2-WL, together with Lemma 2, there is

$$\{\mathbf{c}^{(T)}((i, j)) : i, j \in V, i \neq j\} = \{\mathbf{c}'^{(T)}((i', j')) : i', j' \in V, i' \neq j'\}$$

and

$$\{\mathbf{c}^{(T)}((i, i)) : i \in V\} = \{\mathbf{c}'^{(T)}((i', i')) : i' \in V\}$$

Hence, by the lemma, we have

$$\{\mathbf{B}_{(i,j)}^{(T)} : i, j \in V, i \neq j\} = \{\mathbf{B}'_{(i',j')}^{(T)} : i', j' \in V, i' \neq j'\}$$

and

$$\{\mathbf{B}_{(i,i)}^{(T)} : i \in V\} = \{\mathbf{B}'_{(i',i')}^{(T)} : i' \in V\}$$

Then, since the second-last layer h in the 2-IGN can be written as

$$h(\mathbf{B}) = \alpha \sum_{i,j \in V, i \neq j} \mathbf{B}_{i,j} + \beta \sum_{i \in V} \mathbf{B}_{i,i} \quad (56)$$

there is

$$h(\mathbf{B}^{(T)}) = h(\mathbf{B}'^{(T)}) \quad (57)$$

and finally

$$m \circ h(\mathbf{B}^{(T)}) = m \circ h(\mathbf{B}'^{(T)}) \quad (58)$$

which means the 2-IGN yields identical outputs on the two graphs.

I Direct proof of Corollary 4 (2-IGNs are unable to matching-count patterns of 3 or more nodes)

Proof. The same counterexample as in the proof of Theorem 2 given in Appendix D applies here, as we are going to show below. Note that we only need to consider the non-clique case, since the set of counterexample graphs for the non-clique case is a superset of the set of counterexample graphs for the clique case.

Let \mathbf{B} be the input tensor corresponding to $G^{[1]}$, and \mathbf{B}' corresponding to $G^{[2]}$. For simplicity, we assume in the proof below that $d_0, \dots, d_T = 1$. The general case can be proved in the same way but with more subscripts. (In particular, for our counterexamples, (62) can be shown to hold for each of the d_0 feature dimensions.) Define a set $S = \{(1, 2), (2, 1), (1 + m, 2 + m), (2 + m, 1 + m), (1, 2 + m), (2 + m, 1), (1 + m, 2), (2, 1 + m)\}$, which represents the “special” edges that capture the difference between $G^{[1]}$ and $G^{[2]}$. We aim to show something like this:

$\forall t,$

$$\left\{ \begin{array}{l} \mathbf{B}_{i,j}^{(t)} = \mathbf{B}'_{i,j}{}^{(t)}, \forall (i, j) \notin S \\ \mathbf{B}_{1,2}^{(t)} = \mathbf{B}'_{1+m,2}{}^{(t)}, \\ \mathbf{B}_{2,1}^{(t)} = \mathbf{B}'_{2,1+m}{}^{(t)}, \\ \mathbf{B}_{1+m,2+m}^{(t)} = \mathbf{B}'_{1,2+m}{}^{(t)} \\ \mathbf{B}_{2+m,1+m}^{(t)} = \mathbf{B}'_{2+m,1}{}^{(t)} \\ \mathbf{B}_{1,2+m}^{(t)} = \mathbf{B}'_{1+m,2+m}{}^{(t)}, \\ \mathbf{B}_{2+m,1}^{(t)} = \mathbf{B}'_{2+m,1+m}{}^{(t)}, \\ \mathbf{B}_{1+m,2}^{(t)} = \mathbf{B}'_{1,2}{}^{(t)} \\ \mathbf{B}_{2,1+m}^{(t)} = \mathbf{B}'_{2,1}{}^{(t)} \end{array} \right. \quad (59)$$

If this is true, then it is not hard to show that the 2-IGN returns identical outputs on \mathbf{B} and \mathbf{B}' , which we will leave to the very end. To represent the different cases above compactly, we define a permutation η_1 on $V \times V$ in the following way. First, define the following permutations on V :

$$\kappa_1(i) = \begin{cases} \text{MOD}_{2m}(1 + m), & \text{if } i \in \{1, 1 + m\} \\ i, & \text{otherwise} \end{cases}$$

Next, define the permutation τ_1 on $V \times V$:

$$\tau_1((i, j)) = (\kappa_1(i), \kappa_1(j))$$

and then η_1 as the restriction of τ_1 on the set $S \subset V \times V$:

$$\eta_1((i, j)) = \begin{cases} \tau_1((i, j)), & \text{if } (i, j) \in S \\ (i, j), & \text{otherwise} \end{cases}$$

Thus, (59) can be rewritten as

$$\forall t, \mathbf{B}_{i,j}^{(t)} = \mathbf{B}'_{\eta_1((i,j))}{}^{(t)} \quad (60)$$

Before trying to prove (60), let's define κ_2, τ_2 and η_2 analogously:

$$\kappa_2(i) = \begin{cases} \text{MOD}_{2m}(2 + m), & \text{if } i \in \{2, 2 + m\} \\ i, & \text{otherwise} \end{cases}$$

$$\tau_2((i, j)) = (\kappa_2(i), \kappa_2(j))$$

$$\eta_2((i, j)) = \begin{cases} \tau_2((i, j)), & \text{if } (i, j) \in S \\ (i, j), & \text{otherwise} \end{cases}$$

Thus, by symmetry, (60) is equivalent to

$$\forall t, \mathbf{B}_{i,j}^{(t)} = \mathbf{B}'_{\eta_1((i,j))}{}^{(t)} = \mathbf{B}'_{\eta_2((i,j))}{}^{(t)} \quad (61)$$

Because of the recursive relation (1), we will show (61) by induction on t . For the base case, it can be verified that

$$\mathbf{B}_{i,j}^{(0)} = \mathbf{B}'_{\eta_1((i,j))}^{(0)} = \mathbf{B}'_{\eta_2((i,j))}^{(0)} \quad (62)$$

thanks to the construction of $G^{[1]}$ and $G^{[2]}$. Moreover, if we define another permutation $V \times V$, ζ_1 :

$$\zeta_1((i,j)) = \begin{cases} (\text{MOD}_{2m}(i+m), \text{MOD}_{2m}(j+m)), \\ \quad \text{if } j \in \{1, 1+m\}, i \notin \{2, 2+m\} \\ \quad \text{or } i \in \{1, 1+m\}, j \notin \{2, 2+m\} \\ (i,j), \text{ otherwise} \end{cases} \quad (63)$$

then thanks to the symmetry between (i,j) and $(i+m, j+m)$, there is

$$\mathbf{B}_{i,j}^{(0)} = \mathbf{B}_{\zeta_1((i,j))}^{(0)}, \mathbf{B}'_{i,j}^{(0)} = \mathbf{B}'_{\zeta_1((i,j))}^{(0)}$$

Thus, for the induction to hold, and since σ applies entry-wise, it is sufficient to show that

Lemma 8. *If*

$$\mathbf{B}_{i,j} = \mathbf{B}_{\zeta_1((i,j))}, \mathbf{B}'_{i,j} = \mathbf{B}'_{\zeta_1((i,j))} \quad (64)$$

$$\mathbf{B}_{i,j} = \mathbf{B}'_{\eta_1((i,j))} = \mathbf{B}'_{\eta_2((i,j))}, \quad (65)$$

then

$$L(\mathbf{B})_{i,j} = L(\mathbf{B})_{\zeta_1((i,j))}, L(\mathbf{B}')_{i,j} = L(\mathbf{B}')_{\zeta_1((i,j))} \quad (66)$$

$$L(\mathbf{B})_{i,j} = L(\mathbf{B}')_{\eta_1((i,j))} = L(\mathbf{B}')_{\eta_2((i,j))}, \quad (67)$$

Proof of Lemma 8: Again, by symmetry between (i,j) and $(i+m, j+m)$, (66) can be easily shown.

For (67), because of the symmetry between η_1 and η_2 , we will only prove the first equality. By Maron et al. (2018), we can express the linear equivariant layer L by

$$L(\mathbf{B})_{i,j} = \sum_{(k,l)=(1,1)}^{(2m,2m)} T_{i,j,k,l} \mathbf{B}_{k,l} + Y_{i,j}$$

where crucially, $T_{i,j,k,l}$ depends only on the equivalence class of the 4-tuple (i,j,k,l) .

We consider eight different cases separately.

Case 1 $i, j \notin \{1, 2, 1+m, 2+m\}$

There is $\eta_1((i, j)) = (i, j)$, and $(i, j, k, l) \sim (i, j, \eta_1((k, l)))$, and thus $T_{i,j,k,l} = T_{i,j,\eta_1((k,l))}$. Therefore,

$$\begin{aligned}
L(\mathbf{B}')_{\eta_1((i,j))} &= L(\mathbf{B}')_{i,j} \\
&= \sum_{(k,l)=(1,1)}^{(2m,2m)} T_{i,j,k,l} \mathbf{B}'_{k,l} + Y_{i,j} \\
&= \sum_{\eta_1((k,l))=(1,1)}^{(2m,2m)} T_{i,j,\eta_1((k,l))} \mathbf{B}'_{\eta_1((k,l))} + Y_{i,j} \\
&= \sum_{(k,l)=(1,1)}^{(2m,2m)} T_{i,j,\eta_1((k,l))} \mathbf{B}'_{\eta_1((k,l))} + Y_{i,j} \\
&= \sum_{(k,l)=(1,1)}^{(2m,2m)} T_{i,j,k,l} \mathbf{B}'_{\eta_1((k,l))} + Y_{i,j} \\
&= \sum_{(k,l)=(1,1)}^{(2m,2m)} T_{i,j,k,l} \mathbf{B}_{k,l} + Y_{i,j} \\
&= \mathbf{B}_{i,j}
\end{aligned}$$

Case 2 $i \in \{1, 1+m\}$, $j \notin \{1, 2, 1+m, 2+m\}$

There is $\eta_1((i, j)) = (i, j)$, and $(i, j, k, l) \sim (i, j, \eta_2((k, l)))$, because η_2 only involves permutation between nodes 2 and $2+m$, while i and $j \notin \{2, 2+m\}$. Thus, $T_{i,j,k,l} = T_{i,j,\eta_2((k,l))}$. Therefore,

$$\begin{aligned}
L(\mathbf{B}')_{\eta_1((i,j))} &= L(\mathbf{B}')_{i,j} \\
&= \sum_{(k,l)=(1,1)}^{(2m,2m)} T_{i,j,k,l} \mathbf{B}'_{k,l} + Y_{i,j} \\
&= \sum_{\eta_2((k,l))=(1,1)}^{(2m,2m)} T_{i,j,\eta_2((k,l))} \mathbf{B}'_{\eta_2((k,l))} + Y_{i,j} \\
&= \sum_{(k,l)=(1,1)}^{(2m,2m)} T_{i,j,\eta_2((k,l))} \mathbf{B}'_{\eta_2((k,l))} + Y_{i,j} \\
&= \sum_{(k,l)=(1,1)}^{(2m,2m)} T_{i,j,k,l} \mathbf{B}'_{\eta_2((k,l))} + Y_{i,j} \\
&= \sum_{(k,l)=(1,1)}^{(2m,2m)} T_{i,j,k,l} \mathbf{B}_{k,l} + Y_{i,j} \\
&= \mathbf{B}_{i,j}
\end{aligned}$$

Case 3 $j \in \{1, 1+m\}$, $i \notin \{1, 2, 1+m, 2+m\}$

Analogous to case 2.

Case 4 $i \in \{2, 2+m\}$, $j \notin \{1, 2, 1+m, 2+m\}$

There is $\eta_1((i, j)) = (i, j)$, and $(i, j, k, l) \sim (i, j, \eta_1((k, l)))$, because η_1 only involves permutation between nodes 1 and $1+m$, while i and $j \notin \{1, 1+m\}$. Thus, $T_{i,j,k,l} = T_{i,j,\eta_1((k,l))}$. Therefore, we can apply the same proof as for case 2 here except for changing η_2 's to η_1 's.

Case 5 $j \in \{2, 2+m\}$, $i \notin \{1, 2, 1+m, 2+m\}$
 Analogous to case 4.

Case 6 $(i, j) \in S$
 Define one other permutation on $V \times V$, ξ_1 , as $\xi_1((i, j)) =$

$$\begin{cases} (\text{MOD}_{2m}(i+m), j), & \text{if } \text{MOD}_m(j) = 1, \text{MOD}_m(i) \neq 1 \text{ or } 2 \\ (i, \text{MOD}_{2m}(j+m)), & \text{if } \text{MOD}_m(i) = 1, \text{MOD}_m(j) \neq 1 \text{ or } 2 \\ (i, j), & \text{otherwise} \end{cases}$$

It can be verified that

$$\xi_1 \circ \tau_1 = \eta_1 \circ \zeta_1$$

Moreover, it has the property that if $(i, j) \in S$, then

$$(i, j, k, l) \sim (i, j, \xi_1(k, l))$$

because ξ_1 only involves permutations among nodes not in $\{1, 2, 1+m, 2+m\}$ while $i, j \in \{1, 2, 1+m, 2+m\}$. Thus, we have

$$\begin{aligned} (i, j, k, l) &\sim (\kappa_1(i), \kappa_1(j), \kappa_1(k), \kappa_1(l)) \\ &= (\tau_1(i, j), \tau_1(k, l)) \\ &= (\eta_1(i, j), \tau_1(k, l)) \\ &\sim (\eta_1(i, j), \xi_1 \circ \tau_1(k, l)) \\ &= (\eta_1(i, j), \eta_1 \circ \zeta_1(k, l)), \end{aligned}$$

implying that $T_{i,j,k,l} = T_{\eta_1(i,j), \eta_1 \circ \zeta_1(k,l)}$. In addition, as $\eta_1((i, j)) \sim (i, j)$, there is $Y_{\eta_1((i,j))} = Y_{i,j}$. Moreover, by (64),

$$\mathbf{B}'_{\eta_1 \circ \zeta_1((k,l))} = \mathbf{B}'_{\eta_1((k,l))} = \mathbf{B}_{k,l}$$

Therefore,

$$\begin{aligned} L(\mathbf{B}')_{\eta_1((i,j))} &= \sum_{(k,l)=(1,1)}^{(2m,2m)} T_{\eta_1((i,j)), k, l} \mathbf{B}'_{k,l} + Y_{\eta_1((i,j))} \\ &= \sum_{\eta_1 \circ \zeta_1((k,l))=(1,1)}^{(2m,2m)} T_{\eta_1((i,j)), \eta_1 \circ \zeta_1((k,l))} \mathbf{B}'_{\eta_1 \circ \zeta_1((k,l))} + Y_{\eta_1((i,j))} \\ &= \sum_{(k,l)=(1,1)}^{(2m,2m)} T_{\eta_1((i,j)), \eta_1 \circ \zeta_1((k,l))} \mathbf{B}'_{\eta_1 \circ \zeta_1((k,l))} + Y_{\eta_1((i,j))} \\ &= \sum_{(k,l)=(1,1)}^{(2m,2m)} T_{i,j,k,l} \mathbf{B}_{k,l} + Y_{i,j} \\ &= \mathbf{B}_{i,j} \end{aligned}$$

Case 7 $i, j \in \{1, 1+m\}$ There is $\eta_1(i, j) = (i, j)$ and $(i, j, k, l) \sim (i, j, \eta_2((k, l)))$. Thus, $T_{i,j,k,l} = T_{i,j,\eta_2((k,l))}$, and the rest of the proof proceeds as for case 2.

Case 8 $i, j \notin \{1, 1+m\}$ There is $\eta_1(i, j) = (i, j)$ and $(i, j, k, l) \sim (i, j, \eta_1((k, l)))$. Thus, $T_{i,j,k,l} = T_{i,j,\eta_1((k,l))}$, and the rest of the proof proceeds as for case 4.

□

With the lemma above, (60) can be shown by induction as a consequence. Thus,

$$\mathbf{B}_{i,j}^{(T)} = \mathbf{B}_{\eta_1(i,j)}^{(T)}$$

Maron et al. (2018) show that the space of linear invariant functions on $\mathbb{R}^{n \times n}$ is two-dimensional, and so for example, the second-last layer h in the 2-IGN can be written as

$$h(\mathbf{B}) = \alpha \sum_{i,j=(1,1)}^{(2m,2m)} \mathbf{B}_{i,j} + \beta \sum_{i=1}^{2m} \mathbf{B}_{i,i}$$

for some $\alpha, \beta \in \mathbb{R}$. Then since η_1 is a permutation on $V \times V$ and also is the identity map when restricted to $\{(i, i) : i \in V\}$, we have

$$\begin{aligned} h(\mathbf{B}'^{(T)}) &= \alpha \sum_{(i,j)=(1,1)}^{(2m,2m)} \mathbf{B}'_{i,j}{}^{(T)} + \beta \sum_{i=1}^{2m} \mathbf{B}'_{i,i}{}^{(T)} \\ &= \alpha \sum_{(i,j)=(1,1)}^{(2m,2m)} \mathbf{B}'_{\eta_1((i,j))}{}^{(T)} + \beta \sum_{i=1}^{2m} \mathbf{B}'_{\eta_1((i,i))}{}^{(T)} \\ &= \alpha \sum_{(i,j)=(1,1)}^{(2m,2m)} \mathbf{B}_{i,j}^{(T)} + \beta \sum_{i=1}^{2m} \mathbf{B}_{i,i}^{(T)} \\ &= h(\mathbf{B}^{(T)}) \end{aligned}$$

Therefore, finally,

$$m \circ h(\mathbf{B}^{(T)}) = m \circ h(\mathbf{B}'^{(T)})$$

□

J Specific GNN architectures

In Section 6, we show experiments on synthetic datasets with several related architectures. Here are some explanation for them:

- **LRP- i - j** : Local Relational Pooling with a egonet of depth i and a cropped subtensor of size j along the axis of adjacency matrix. In our experiments, we take $i = 1, j = 4$. Hence, the vectorized subtensor (or submatrix, as the graph is unattributed) is of size $4 \times 4 = 16$. The number of hidden dimensions is 128. The non-linearities are in $\{\text{ReLU}, \tanh\}$. The models are trained using the Adam optimizer Kingma and Ba (2014) with learning rate 0.1. The number of hidden dimensions is searched in $\{1, 8, 16, 64, 128\}$.
- **2-IGN**: 2nd-order Invariant Graph Networks proposed by Maron et al. (2018). In our experiments, we take 8 hidden dimensions for invariant layers and 16 hidden dimensions for output multi-layer perceptron. The models are trained using the Adam optimizer with learning rate 0.1. The numbers of hidden dimensions are searched in $\{(16, 32), (8, 16), (64, 64)\}$.
- **GCN**: Graph Convolutional Networks proposed by Kipf and Welling (2016). In our experiments, we adopt a 4-layer GCN with 128 hidden dimensions. The models are trained using the Adam optimizer with learning rate 0.01. The number of hidden dimensions is searched in $\{8, 32, 128\}$. Depth is searched in $\{2, 3, 4, 5\}$.

- **GIN**: Graph Isomorphism Networks proposed by [Xu et al. \(2018a\)](#). In our experiments, we adopt a 4-layer GIN with 32 hidden dimensions. The models are trained using the Adam optimizer with learning rate 0.01. The number of hidden dimensions is searched in {8, 16, 32, 128}.
- **sGNN**: Spectral GNN with operators from family $\{\mathbf{I}, \mathbf{A}, \min(\mathbf{A}^2, 1)\}$. In our experiments, we adopt a 4-layer sGNN with 128 hidden dimensions. The models are trained using the Adam optimizer with learning rate 0.01. The number of hidden dimensions is searched in {8, 128}.

For GCN, GIN and sGNN, we always train four variants for each architecture, depending on whether Jump Knowledge [Xu et al. \(2018b\)](#) or Batch Normalization [Ioffe and Szegedy \(2015\)](#) is included or not. All models are trained for 100 epochs. Learning rates are searched in {1, 0.1, 0.05, 0.01}. We pick the best model with the lowest MSE loss on validation set to generate results.

K Experiment results

Table 2: Test MSE loss for all models with chosen parameters as specified in Appendix J. We run each model for five times and pick top 1 / top 3 (median) results for Table 1. Note that each of GCN, GIN and sGNN has four variants. The reported rows in Table 1 are bolded.

Dataset: Erdős-Renyi										
	3-Star (C)					Triangle (M)				
LRP-1-4	6.74E-03	1.63E-02	1.10E-01	1.58E-01	6.79E-03	2.05E-02	1.50E-02	1.83E-03	1.15E-03	1.51E-03
2-IGN	1.68E-01	3.04E+02	1.59E+01	5.70E+01	7.36E+00	8.90E-01	7.22E+00	9.63E-01	1.70E+00	7.22E+00
GCN	1.42E+02	1.36E+02	1.51E+02	1.36E+02	1.51E+02	7.24E+00	7.24E+00	7.24E+00	7.24E+00	7.22E+00
GCN+JK	2.59E+02	1.45E+02	1.86E+02	2.15E+02	2.35E+02	6.07E+00	4.98E+00	5.32E+00	6.34E+00	6.40E+00
GCN+BN	5.67E+04	3.74E+04	3.55E+04	4.97E+04	1.85E+05	5.85E+02	5.17E+02	3.73E+02	3.53E+02	1.89E+03
GCN+JK+BN	2.89E+02	3.06E+02	2.96E+02	3.00E+02	2.97E+02	1.09E+01	7.23E+00	6.98E+00	7.21E+00	7.22E+00
GIN	2.95E-01	3.04E+02	3.04E+02	3.04E+02	3.04E+02	9.64E-01	7.22E+00	7.22E+00	7.22E+00	7.22E+00
GIN+JK	1.07E-01	2.66E-01	1.30E-01	5.05E-02	5.93E-02	9.31E-01	9.05E-01	9.30E-01	9.20E-01	9.16E-01
GIN+BN	2.27E+02	1.27E+03	2.31E+02	1.65E+02	3.37E+02	1.34E+01	7.34E+01	2.80E+01	4.22E+00	1.67E+01
GIN+JK+BN	7.14E+02	3.03E+02	1.88E+02	5.94E+02	2.96E+04	4.73E+01	3.12E+00	5.55E+00	1.02E+01	4.95E+01
sGNN	3.10E+00	2.66E+00	7.36E-01	1.17E+00	2.40E+00	8.27E-01	8.46E-01	6.80E-01	7.09E-01	3.03E+00
sGNN+JK	1.29E+02	7.39E+01	2.80E+03	5.45E+02	6.32E+01	4.92E+00	5.30E+00	1.22E+01	1.07E+01	4.56E+00
sGNN+BN	1.17E+04	2.05E+03	6.05E+01	4.09E+02	3.54E+02	2.90E+02	1.88E+02	7.98E+01	8.25E+02	9.46E+01
sGNN+JK+BN	3.01E+02	3.02E+02	3.12E+02	6.74E+07	3.02E+02	7.23E+00	6.83E+00	1.36E+05	6.46E+02	7.21E+00

Dataset: Random Regular										
	3-Star (C)					Triangle (M)				
LRP-1-4	8.89E-04	8.43E-03	7.20E-04	5.38E-03	5.94E-04	2.33E-03	2.83E-01	3.40E-03	4.40E-01	3.61E-03
2-IGN	3.02E+02	3.05E+02	3.10E+02	1.49E+02	1.93E+01	2.49E+00	9.51E+00	2.47E+00	5.61E+00	9.51E+00
GCN	8.85E+02	8.98E+02	8.32E+02	8.93E+02	8.38E+02	2.01E+01	2.01E+01	2.01E+01	2.01E+01	2.01E+01
GCN+JK	8.92E+02	8.96E+02	8.80E+02	8.98E+02	8.91E+02	1.97E+01	1.82E+01	1.93E+01	1.97E+01	1.98E+01
GCN+BN	1.08E+05	1.34E+04	4.09E+04	3.03E+05	1.30E+05	1.66E+03	6.29E+03	1.15E+03	5.21E+03	7.31E+01
GCN+JK+BN	1.49E+04	8.83E+02	8.70E+02	8.88E+02	9.83E+02	4.29E+01	1.94E+01	1.78E+01	1.72E+01	1.94E+01
GIN	3.38E-01	8.99E+02	8.99E+02	8.99E+02	8.99E+02	2.01E+01	2.01E+01	2.01E+01	2.01E+01	2.01E+01
GIN+JK	4.32E-01	1.47E-01	1.72E-01	1.18E-01	1.37E-01	4.47E+00	4.44E+00	4.43E+00	4.47E+00	4.47E+00
GIN+BN	8.99E+02	8.99E+02	5.64E+02	5.78E+02	8.99E+02	5.25E+06	2.01E+01	2.09E+02	2.01E+01	2.01E+01
GIN+JK+BN	3.58E+03	8.73E+03	6.18E+03	2.56E+03	2.03E+03	1.48E+03	1.07E+01	1.33E+01	6.42E+01	1.64E+01
sGNN	7.50E+00	4.45E+01	8.98E+00	1.86E+02	7.82E+01	3.70E+00	6.58E+00	4.17E+00	1.09E+01	4.15E+00
sGNN+JK	6.33E+02	5.40E+02	7.33E+02	1.81E+04	7.33E+02	1.38E+01	1.51E+01	2.29E+01	4.02E+03	1.52E+01
sGNN+BN	4.53E+02	3.93E+02	1.45E+02	2.06E+03	2.29E+03	1.02E+02	5.16E+04	2.25E+03	5.87E+02	2.14E+03
sGNN+JK+BN	4.43E+04	8.99E+02	8.90E+02	2.76E+10	8.99E+02	1.99E+01	2.04E+01	2.24E+01	3.63E+08	2.00E+01